People's Democratic Republic of Algeria
Ministry of Higher Education and Scientific Research

University M'Hamed BOUGARA – Boumerdes

Institute of Electrical and Electronic Engineering

Department of Power and Control Engineering

Final Year Project Report Presented in Partial Fulfilment of the Requirements for the Degree of

MASTER

In **Power Engineering**

Option: **Power Engineering**

Title:

Modeling and Control of VSC-Based High Voltage Direct Current Transmission System

Presented by:

- **Abderrahim Aimane MEFLAH**
- **Hicham Abderrahim SAHBI**

Supervisor:

- **Abdelkarim Ammar**

2021/2020

Acknowlegement

First of all, we would like to thank Allah the Almighty for giving us knowledge, health and will to accomplish this study during a world pandemic.

We would like to express our great gratitude to our supervisor: **Dr.AMMAR Abdelkarim** for his guidance, help and support throughout the project and always being there for us whenever we needed him. We couldn't have done it without him.

Last but not least, we are grateful to our parents for their encouragement, guidance and unconditional support, both psychologically and financially during our years of education; May Allah bless them.

Abstract

VSC-Based High Voltage Direct Current (VSC-HVDC) systems have the ability to control rapidly the transmitted active power and independently exchange reactive power with transmissions systems. The present work investigates the modeling and control of a high-voltage direct current (HVDC) transmission system based on three-level NPC converters. A feed-forward current control strategy using PI controllers has been performed in order to achieve a decoupled indirect active and reactive power control. By using this control strategy, not only the powers can be controlled independently but also the dynamic response time can be shortened. Furthermore, PI controllers are implemented for out loops control. In this work, Modeling and Simulation studies of a 3MW/±50kV back-to-back VSC-HVDC are presented. Different tests have been performed to confirm the satisfactory performance of the proposed system under active and reactive power variations and DC pole-to-pole Disturbances.

Keywords : HVAC, HVDC, LCC, VSC, Vector Controller, Simulink .

Contents

List of Figures

List of Tables

List of Abbreviations

VSC	*Voltage source Converter*
CSC	*Current Source Converter*
DCC	*Direct Current Control*
FFT	*Fast Fourier Transform*
GTOs	*Gate Turn-Off Thyristors*
HVAC	*High Voltage Alternating Current*
HVDC	*High Voltage Direct Current*
IGBT	*Insulated Gate Bipolar Transistor*
IGCT	*Insulated Gate Commutated Thyristor*
LCC	*Line Commutated Converter*
PCC	*Point of Common Coupling*
PLL	*Phase Lock Loop*
PI control	*Proportional plus Integral control*
MMC	*Mulit-Module Converter*
PWM	*Pulse Width Modulation*
CC	*Current Control*
VCC	*Vector Current Control*
APC	*Active Power Controller*

PRC *Reactive Power Controller*

DVC *Direct Voltage Controller*

SCR *Short Circuit Ratio*

General Introduction

To meet the growing energy demand, the global annual electricity generation is anticipated to surpass 38,000 TWh by 2040 compared to 24,000 TWh in 2016. As a result, the European high-voltage alternating-current (HVAC) grid is operating very close to its limits. The contribution of renewable energy sources is expected to approach 56% of the total generation mix by 2050 compared to 22% today. Wind-capacity grows at 5.7% year-on-year to 2050, with annual average deployment of 147GW. Growth for PV is 5.3% year-on-year, or average annual deployment of 246GW[1]. To ensure effective energy generation, transmission, and distribution, this necessitates constant network infrastructure improvement and huge investments. That is, many large-scale renewable energy power plants are located far from main demand centers, necessitating efficient bulk energy transmission over extremely long distances. Similar efficient and cost-effective transmission criteria is required for offshore wind farms that have increased their market share recently, especially in Northern/Western Europe.

In contrast, the interconnection of regional and national electricity markets is expanding globally for energy trading and raising the security of supply level. For example, the EU recently set a target for each country to attain 15% of its installed capacity in interconnected capacity with neighboring markets by 2030 [2]. Bulk energy transmission/ interconnection is feasible using both high voltage alternating current (HVAC) and high voltage direct current (HVDC) links. Because of their technological and economic superiority over HVAC systems for long-distance transmission, HVDC systems are playing an increasingly important role in energy transmission.

In a HVDC transmission system, the converter serves as an interface between the DC and AC networks, converting the two signals. The converter might function as a rectifier, converting an AC signal to a DC signal, or as an inverter, converting a DC signal back to an AC signal. Development of power electronics has innovated the converter technology, enhancing the quality of the output signal and the stability of HVDC system control.Line-Commutated Converter (LCC) technology utilizes thyristors for power conversion. However, The Voltage Source Converter (VSC) technology utilizes gate-turn-off thyristors (GTOs) or in most industrial cases insulated gate bipolar transistors (IGBTs) for switching.

VSC-HVDC, controlled by pulse width modulation (PWM), can supply power to both active and passive electrical systems. The introduction of VSC and PWM makes possible fast and flexible control of power flow and more convenient operation of power systems. Besides, this advancement, compared with conventional (LCC) HVDC, mitigates

harmonics in AC current and AC voltage greatly and improves power factors of the connected AC systems[3]. VSC-HVDC, in recent years, have successfully been commercially commissioned in such fields as supplying power to remote isolated loads, empowering urban centers, connecting distributed generation sources, linking two asynchronous electrical power systems, improving power quality.

In this thesis a model of a VSC-based HVDC using PWM Technology is developed. A mathematical model of the control system based on the relationships between voltage and current is described for the VSC. A control system is developed combining an inner current loop controller and outer dc voltage controller. The vector control strategy is also studied. We tested the system under DC fault .

This report is organized as follow:

- The 1st chapter provides the historical background of HVDC transmission in the 1st part. Then a comparison between the HVDC and HVAC systems. Different applications of the HVDC system are listed .
- The 2nd chapter describes the HVDC converter arrangements. It then explains the main structure of a VSC-HVDC transmission system. At the end we provided a comparison between the classical HVDC and the VSC .
- The 3rd chapter deals with the control system, first we discuss the converter control principle. Then the control strategies we talked about all the control strategies and we gave a comparison between them. We discuss in details the vector current principle .
- The 4th chapter is dedicated to the faults in the DC system, Pole-to-Ground fault and pole-to-pole fault. The obtained results are discussed in the last chapter .

Chapter 1

Introduction

1.1 Historical Background of HVDC Transmission

Today, the war of currents between Thomas Edison and Nicolas Tesla has evolved into a war of voltages. In the literature, technical arguments on high voltage AC and DC systems have been recorded. Thomas Edison (1847–1931) and Nicolas Tesla (1856–1943) were pioneers of direct (DC) and alternating current (AC) power systems. On September 4, 1882 Edison's 110V DC lightened the Pearl Street in New York and Tesla's two-phase 240 V,25Hz AC lit the World Columbian exposition fair Chicago on 16 November, 1893 .Edison made DC motor and Tesla designed AC motor. General Electric Company backed Edison's direct current (DC) system, whereas Westinghouse Company backed Tesla's flexible alternating current (AC) system. AC won over the DC due to its high voltage, low loss power transmission capabilities, also due to the invention of the transformer that allowed using more and higher voltage levels and led to economic transport of electric power over longer distances. Furthermore, it is convenient producing rotating fields for electrical machines using AC . Three-phase 50/60 Hz systems remained in use for a few decades, but after the invention of DC converters in the 1930s, utilities resumed HVDC line construction to reap the benefits of lower line losses over greater distances. Earlier DC systems had no voltage transformation facility like AC transformers. Rene Thury, a Swiss engineer, proposed connecting multiple DC generators in series to improve transmission voltage and using DC batteries at the terminal station to distribute power at specified voltage levels. First (530 kW) 120 km long DC line was built using series connected generators based upon Thury Schemes [4]. DC–DC converters (transformers) first appeared in the 1920s and 1930s as mercury arc converters [5], then as semiconductor Thyristors in the 1970s and IGBTs in the 1990s. DC lines used series connected DC generators (Thury) from 1882 to 1925, mercury rectifiers from1925 to1970, Thyristors from 1970s and IGBTs from 1990s to date. The first commercial HVDC link was built by ABB in Sweden by 1954 after years of experimentation. The Gotland 1 link spanned 98 km, carrying 20 MW at 100 kV [2]. HVDC transmission is now more cost-effective than HVAC due to the development of gate-turn off Thyristors (GTOs) and integrated gate commutated Thyristors (IGCT). First 500 kV HVDC line using Thyristors and first 200 kV line using IGBTs was built in 1970s and in 2002 in USA. Thyristor based HVDC systems have grown to 800 kV and IGBTs based HVDC systems to 300 kV voltage levels today [6]. After a several-decade hiatus, the war of currents between Edison's bipolar DC and Tesla's two-phase AC systems resurfaced in the 1990s as a war of voltages between China and India.

The main difference between thyristors and IGBTs in operation of the power converter is the turn-off capability of the latter. This seemingly small difference has completely revolutionised the world of HVDC: the use of IGBTs instead of thyristors is not a developm-ent comparable to the transition from mercury-arc valves to thyristor valves, but a rupture that required a complete change of the layout and design philosophy of the converter stations, greatly expanding the range of applications of HVDC [7]. Converters with IGBTs did not replace converters with thyristors: both systems exist because their field of application is not the same. To distinguish between both systems, the term Current Source Converter (CSC) HVDC is used for the thyristor converter HVDC, and Voltage Source Converter (VSC) for the IGBT converter HVDC. Alternatively, they are referred

to as respectively line-commutated and self-commutated converters. The first commercial installation of VSC HVDC was commissioned in 1999 on the island of Gotland, Sweden. This system has a rated power of 50 MW at a DC voltage of ± 80 kV [8]. HVDC systems are at the moment being planned and implemented in a bigger and faster way than what was expected, Tables 1.1 show lists of some operating HVDC systems with different technologies [9].

System	Year Commissioned	System's Capacity[MW]
Gotland	1970	20
Skagerrak	1976	500
Cahora Bassa	1977	1930
Inga-Kolwezi	1982	560
CU Project	1979	1000
Neison River	1985	2000
Itaipu	1984-90	3150
Pacific Intertie	1970	1440
Intermountain	1986	1920
Fenno-Skan	1989	500
Rihand Delhi	1990	1568
Quebec-New England	1992	2000
New Zealand	1992	560
Baltic Cable	1994	600
Chandarpur-Paghe	1998	1500
SwePol	2000	600
Brazil-Argentina (Inter1)	2000	1100
3 Georges-Changzhou	2003	3000
3 Georges-Guandong	2004	3000
Norned	2008	700
Xiangjiaba-Shangahai	2010	6400
Hulunbeir-Liaoning	2010	3000
SAPEI	2011	1000
Rio Madeira	2012	3150
Jinping-Sunan	2013	7200
Jinbei-Nanjing	2017	8000
North-East Arga	2017	6000
Jiuquan-Hunan	2017	8000
Changji-Guquan	2017-18	12000

Table 1.1: HVDC classic operating and planned projects

System	Year Commissioned	System's Capacity[MW]
Hallsjon	1997	3
Gotland	1999	50
Tjaereborg	2000	7.2
Eagle Pass	2000	36
Cross sound Cable	2002	330
Troll A 1 and 2	2005	88
Estlink	2006	350
Valhall	2011	78
East West Interconnector	2012	500
Mackinac	2014	200
DolWin1	2015	800
Nordbalt	2015	700
DolWin2	2015	900
Maritme Link	2017	500
Baltic Cable	1994	600
Chandarpur-Paghe	1998	1500
SwePol	2000	600
Caithness Moray HVDC Link	2018	1200
3Johan Sverdrup	2019	100
IFA2 HVDC Transmission Link	2020	1000
Nordlink	2020	1400
NSL	2021	1400

Table 1.2: HVDC light operating and planned projects.

1.2 HVDC vs HVAC

High voltage (HV) is a preferable option to be used in the interconnection instead of medium voltage because it leads to a decrease in line losses. The use of HVDC transmission over long distances provides several technical advantages when compared to HVAC. In comparing an HVAC versus an HVDC connection it is vital to highlight the technical concerns with each system. The first point is stability. Although there are three different limits to the HVAC connection type, (voltage regulation limit, stability limit, and thermal limit), the HVDC connection type only has one; the thermal limit. Whereas the HVAC connection type suffers from reactive power loss due to the existence of capacitance and inductance in the transmission lines, there is no reactive power loss in the HVDC connection type. These losses also depend significantly on the type of conductor used, the length and the cross section of the line and the type of current (AC or DC). DC flows through the entire section of the wire while AC tends to flow towards its surface, which causes the skin effect (Fig.1.1). This reduces the "effective" cross section and thus increases the resistance and power losses [10]. Current carrying capacity is another concern in the HVAC connection type, although this is not a problem with the HVDC connection

type. However, the most essential technical point to be compared between the HVAC and HVDC connection types is the power flow control. The power flow control in the HVAC connection type requires external equipment such as a phase shifter transformer, and a unified power flow control (UPFC), whereas the power flow control in the HVDC connection type can be managed by changing the current direction or voltage polarity [11].

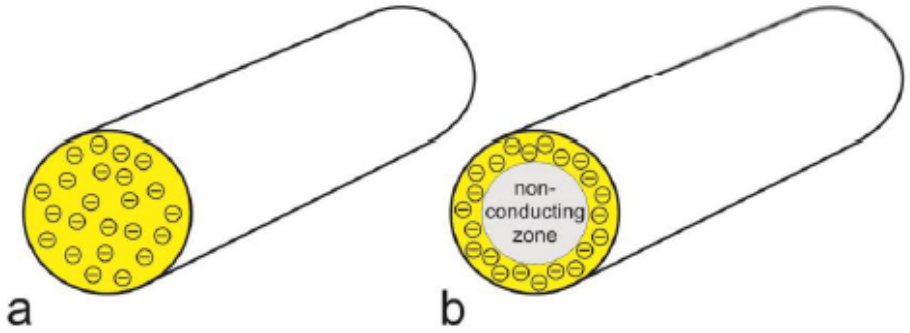

Figure 1.1: DC (a) and AC (b) flow in a conductor; the skin effect.

The economical comparison between the HVAC and HVDC connection types is significant due to the overall cost. DC transmission losses/costs are substantially lower than HVAC due to the absence of transmission line capacitive/reactive charging effects. This confines the main HVDC transmission losses to line-resistive losses, and omits the necessity for expensive, fast, AC line-reactive compensators [12]. DC transmission can thus be employed efficiently for very long transmission distances exceeding 3000 km as of 2018, compared to 1049 km for point-to point HVAC [13]. It also requires fewer cables/conductors and utilizes the full lines transmission capacity up to their thermal limits. This reduces the required cross-sectional area for DC cables and consequently the transmission cost [2]. HVDC cables require less material since they need only one power line in order to transport electricity. An HVAC link needs three power lines to carry the same power. HVDC lines also use less space for their right of way ROW (i.e. the required horizontal ground clearance distance) on land in comparison with HVAC lines, for both overhead and underground bulk power transmission options . The capacitance between the active conductors and the surrounding earth or water restricts the length of the HVAC cables. If the HVAC cable is too long, the reactive power consumed by the cable would absorb the entire current carrying capacity of the conductor and no usable power would be transmitted .

Having said that, the costly rectifier and inverter stations for AC/DC and DC/AC conversions are not required in HVAC applications, significantly add to the overall HVDC transmission cost. That is, DC transmission fixed cost (stations and equipment) is substantially greater compared to AC, yet line costs and losses are highly skewed in the favour of DC. Thus establishing a breakeven distance for both technologies after which DC transmission becomes economically preferable. The HVDC breakeven distance estimations vary but typical ranges expand between 300 km and 800 km for overhead lines and 50 km to 100 km for offshore/underground cable links, Fig. 1.2.(a) qualitatively

summarizes the cost evolution of HVAC vs HVDC converters with distance, indicating breakeven points. This variability is related to individual project conditions (e.g. MW/kV rating, transmission terrain and local policies).

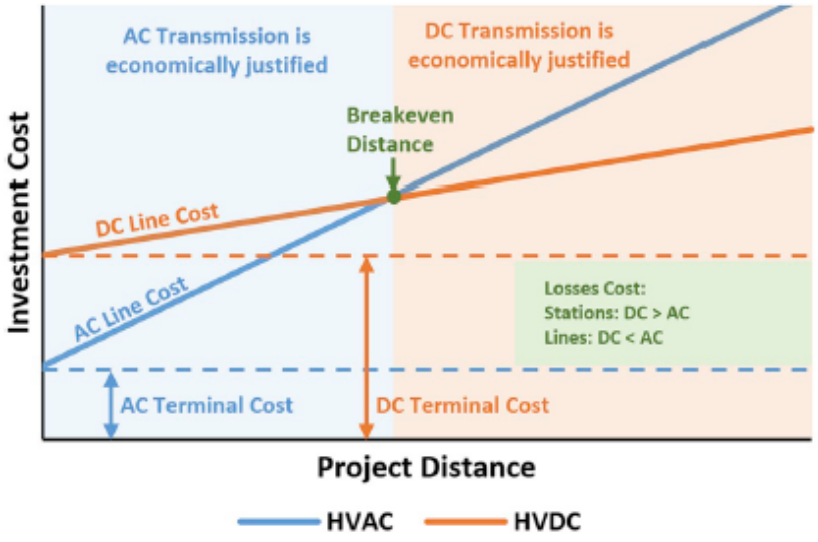

(a)

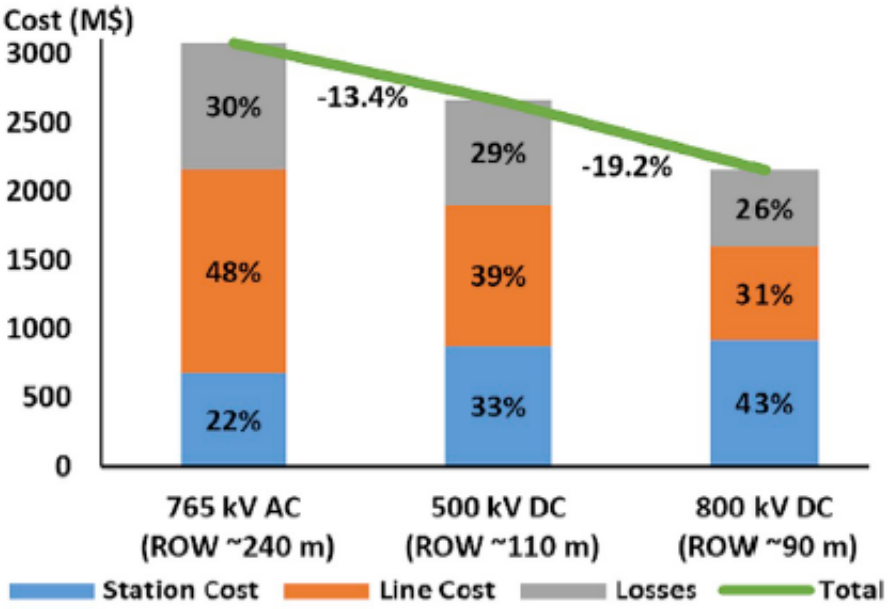

(b)

Figure 1.2: HVAC vs. HVDC cost comparison: (a) qualitative breakeven distance assessment. (b) Cost and ROW estimation for a generic 6000 MW transmission for 2000 km.

Fig. 1.3 (table) summarizes the main comparison points between HVAC and HVDC transmission. Fig.1.2.(b) provides an example from ABB, comparing the costs of different transmission alternatives for a 6000 MW/2000 km link [14 - 2].

Transmission Type		HVAC	HVDC
Cables/Lines	Number of Conductors	Higher (3-phase conductors, lower individual ratings, cumulatively more expensive)	Lower
	Utilization	Limited by skin-effect (although bundled conductors are used to limit it)	Full up to thermal limits
	Losses	Higher (mainly resistive and reactive, requiring expensive line-capacitance compensators)	Lower (mainly resistive and corona losses)
	ROW	Higher (could exceed ×3 times of HVDC) [20]	Lower
Maximum Implemented 2018 Distance	Lower (1049 km: Yuheng-Weifang link in China [17,18])	Higher (3324 km: Changji-Guquan link in China [16])	
Meshed Grids	Availability	Widespread on a global scale	Currently limited with significant predicted growth
	Protective Equipment	Well-Developed UHV Circuit Breakers	Extensive R&D effort to develop HVDC Breakers and/or converters fault blocking capability
Substations	Cost	Significantly Lower	Higher (converter stations)
	Losses [21]	Low transformer and HV equipment losses (0.3% in AC double circuit)	Higher station losses (could exceed 1% for VSC)
Economic Viability		UG Cables < 50–100 km Overhead Line < 300–800 km	(Point-to-Point Links)

Figure 1.3: Technical comparison summary between HVAC and HVDC transmission.

1.3 HVDC Applications

HVDC transmission applications can be divided into several basic categories. Although the reasoning for selecting HVDC is frequently economic, there may be other reasons for its selection. HVDC may be the only feasible way to interconnect two asynchronous networks, reduce fault currents, utilize long cable circuits, bypass network congestion, share utility rights-of-way without degradation of reliability and to mitigate environmental concerns. In all of these applications, HVDC nicely complements the ac transmission system.

1.3.1 Long Distance Bulk Power Transmission

Higher power transfers are possible over longer distances using fewer lines with HVDC transmission than with ac transmission. Typical HVDC lines utilize a bipolar configuration with two independent poles. Bipolar HVDC lines are comparable to a double circuit ac line since they can operate at half power with one pole out of service but require only one-third the insulated sets of conductors as a double circuit ac line. The controllability of HVDC links offers firm transmission capacity without limitation due to network congestion or loop flow on parallel paths. Controllability allows the HVDC to 'leap-frog' multiple 'choke-points' or bypass sequential path limits in the ac network. Therefore, the utilization of HVDC links is usually higher than that for EHV ac transmission lowering the transmission cost per MWh. This controllability can also be very beneficial for the parallel transmission as well since, by eliminating loop flow, it frees up this transmission capacity for its intended purpose of serving intermediate load and providing an outlet for local generation.

1.3.2 Cable Transmission

Unlike the case for ac cables, there is no physical restriction limiting the distance or power level for HVDC underground or submarine cables. Underground cables can be used on shared ROW with other utilities without impacting reliability concerns over use of common corridors. For underground or submarine cable systems there is considerable savings in installed cable costs and cost of losses when using HVDC transmission. Depending on the power level to be transmitted, these savings can offset the higher converter station costs at distances of 40 km or more. Furthermore, there is a drop-off in cable capacity with ac transmission over a distance due to its reactive component of charging current since cables have higher capacitances and lower inductances than ac overhead lines. Although this can be compensated by intermediate shunt compensation for underground cables at increased expense, it is not practical to do so for submarine cables. With a cable system, the need to balance unequal loadings or the risk of post-contingency overloads often necessitates use of a series-connected reactors or phase shifting transformers. These potential problems do not exist with a controlled HVDC cable system. Extruded HVDC cables with prefabricated molded joints used with VSC based HVDC transmission are lighter, more flexible and easier to splice than the mass-impregnated (MI), oil-paper cables used for conventional HVDC transmission thus making them more conducive for land cable applications where transport limitations and extra splicing costs can drive up installation costs. The lower cost cable installations made possible by the extruded HVDC cables and prefabricated joints makes long distance underground transmission economically feasible for use in areas with rights-of-way constraints or subject to permitting difficulties or delays with overhead lines.

1.3.3 Asynchronous Ties

Some applications need the use of reliable HVDC stations as the only choice for connecting two asynchronous AC power systems in different countries or within the same country, as in Japan (with both 50/60 Hz systems) and the United States (with asynchronous 60 Hz systems) [2] . The asynchronous interconnection allows interconnections of mutual benefit while providing a buffer between the two systems. Often these interconnections use back-to-back converters with no transmission line. Asynchronous HVDC links act as an effective “firewall” against propagation of cascading outages in one network from passing to another network. Many asynchronous interconnections exist in japan (with both 50/60

Hz systems) and North America between the eastern and western interconnected systems, between the Electric Reliability Council of Texas (ERCOT) and its neighbors, e.g., Mexico and the Southwest Power Pool (SPP), and between Quebec and its neighbors, e.g., New England and the Maritimes. The August 2003 northeast blackout provides an example of the “firewall” against cascading outages provided by asynchronous interconnections. As the outage expanded and propagated around the lower Great Lakes and through Ontario and New York it stopped at the asynchronous interface with Quebec. Quebec was unaffected, the weak ac interconnections between New York and New England tripped, but the HVDC links from Quebec continued to deliver power to New England.

Interconnections between asynchronous networks are often at the periphery of the respective systems where the networks tend to be weak relative to the desired power transfer. Higher power transfers can be achieved with improved voltage stability in weak system applications using capacitor commutated converters. The dynamic voltage support and improved voltage stability offered by VSC based converters permits even higher power transfers without as much need for ac system reinforcement. VSC converters do not suffer commutation failures allowing fast recoveries from nearby ac faults. Economic power schedules which reverse power direction can be made without any restrictions since there is no minimum power or current restrictions.

1.3.4 Offshore Transmission

Self-commutation, dynamic voltage control and black-start capability allow compact VSC HVDC transmission to serve isolated loads on islands or offshore production platforms over long distance submarine cables. This capability can eliminate the need for running expensive local generation or provide an outlet for offshore generation such as that from wind. The VSC converters can operate at variable frequency to more efficiently drive large compressor or pumping loads using high voltage motors. Large remote wind generation arrays require a collector system, reactive power support and outlet transmission.
Transmission for wind generation must often traverse scenic or environmentally sensitive areas or bodies of water. Many of the better wind sites with higher capacity factors are located offshore. VSC based HVDC transmission not only allows efficient use of long distance land or submarine cables but also provides reactive support to the wind generation complex and interconnection point.

1.3.5 Power Delivery to Large Urban Areas

Power supply for large cities depends on local generation and power import capability. Local generation is often older and less efficient than newer units located remotely. Often, however, the older, less-efficient units located near the city center must be dispatched out-of-merit because they must be run for voltage support or reliability due to inadequate transmission. Air quality regulations may limit the availability of these units. New transmission into large cities is difficult to site due to right of way limitations and land use constraints. Compact VSC-based underground transmission circuits can be placed on existing dual-use rights-of-way to bring in power as well as to provide voltage support allowing a more economical power supply without compromising reliability. The receiving terminal acts like a virtual generator delivering power and supplying voltage regulation and dynamic reactive power reserve. Stations are compact and housed mainly indoors making siting in urban areas somewhat easier. Furthermore, the dynamic voltage support offered by the VSC can often increase the capability of the adjacent ac transmission[15].

1.4 HVDC market overview

HVDC global capacity has well exceeded. Further growth is dependent on market demand and technology development.More than half of this capacity (52%) is internal in Asia (i.e. both sending and receiving ends are located in Asia). This market domination is mainly influenced by China and then India as key market players. Many HVDC projects in that area are constructed to transmit bulk energy from distant generation sites/ renewable energy sources to major load centers over very long distances due to the vast geographic sparsity of these countries. Several recent projects in China are highly rated at 6400 MW/±800 kV , with some links already exceeding 12,000MW [16]. This development has pushed the limits of available technologies and encouraged manufacturers to invest in higher-rating equipment and testing facilities. For instance, main HVDC suppliers (ABB Siemens) have announced their new 1100 kV single-phase transformer units for Ultra HVDC (UHVDC) applications [16]. The average capacity for internal Asian projects is around 4000 MW, which is significantly ahead of other regions (e.g. 1600MW for Central & South America, compared to 1500MW for North America and around 1100MW in Europe). The evolving Chinese dominance in particular over the global HVDC capacity is evident in Fig. 1.4, which illustrates the main markets share between 2010 and 2017. Similar trends are persistent over longer periods; though graphical illustration is presented for this period in particular due to its contribution to the rapid HVDC expansion presented by Fig.1.5, especially in China .

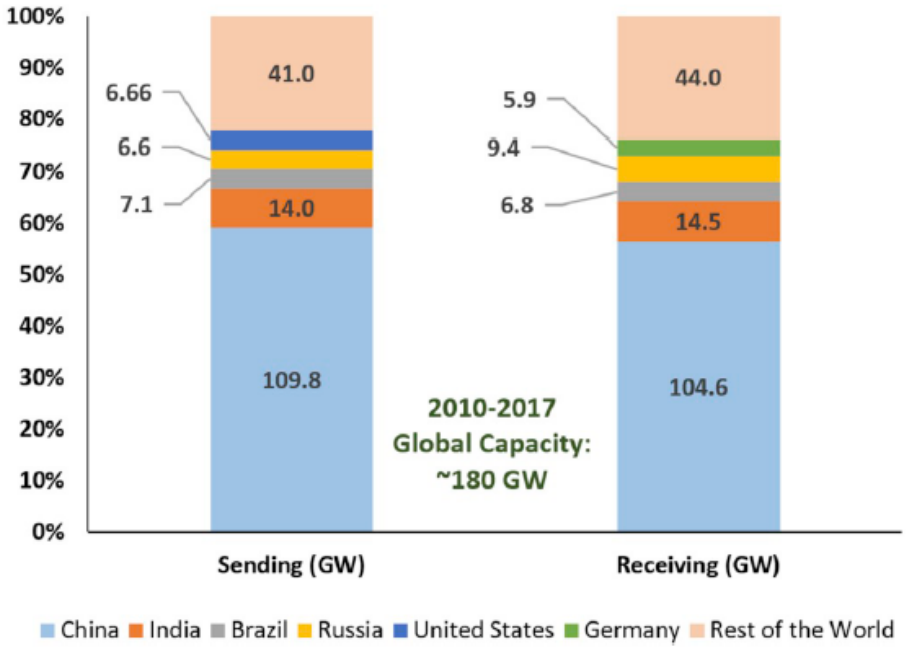

Figure 1.4: HVDC global capacity distribution between 2010 and 2017, based on raw dataset.

The largest number of recorded projects lays in Europe. Yet the internal European projects capacity accounts for 22 % of global HVDC projects compared to the Asian capacity dominance illustrated earlier due to the demand distribution and geographical

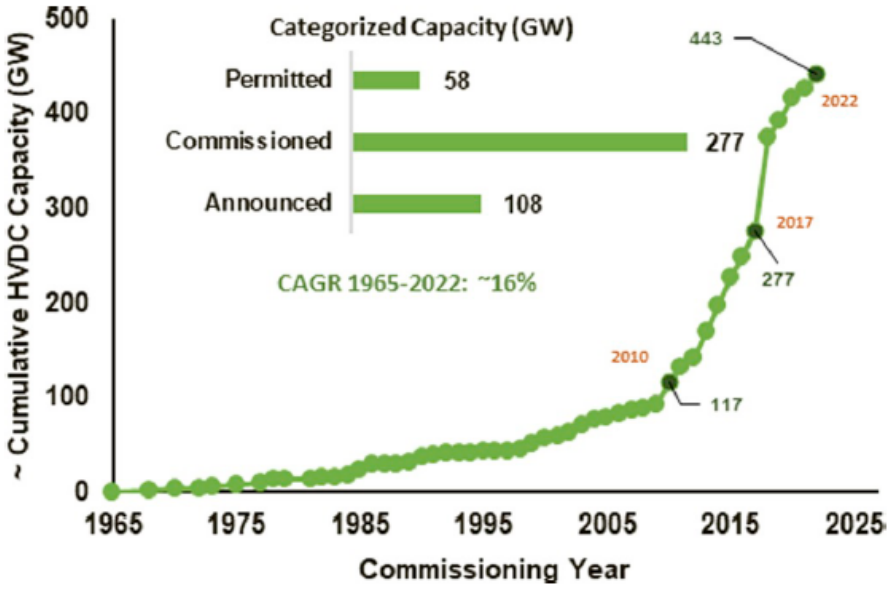

Figure 1.5: Capacity evolution of HVDC interconnectors based on BNEF raw dataset.

variations. That is, constructing expensive UHVDC links with very high transmission capacities is only justified when there is a matching demand in importing areas. In this context, the moderate average capacity of European HVDC links compared to that of China is reasonable, considering the absence of the need case for very high power transfer or very long distance links. Instead, cross-borders point-to-point HVDC links with 1–2GW capacity are common in Europe as part of EU incentives and initiatives to increase the interconnection of markets and security of supply [12]. In fact, several HVDC links are supported both financially and regulatory by the EU under the"Projects of Common Interest" pillar with several defined priority energy corridors such as the"Priority Corridor Northern Seas Offshore Grid" and "Priority Corridor Baltic Energy Market Interconnection Plan". These plans, including both onshore and offshore projects, serve the EU target of achieving its energy interconnection capacity target of (15%)relative to the member states installed capacity) by 2030 [2], while supporting broader utilization of available, sparse, renewable energy sources. This European trend for interconnection of electricity markets is intended to help facilitate proposed plans to reduce nuclear and thermal based generation and to replace it with renewable energy, mainly offshore wind and PV [2].

1.5 Some existing HVDC projects

- The Xiangjiaba-Shanghai ultrahigh voltage direct current (UHVDC) link is the world's first UHVDC connection, one of the longest transmission projects in the world with a length of 1,980km. The transmission line carries electricity generated by the Xiangjiaba hydroelectric power plant in the Sichuan province to Shanghai. Developed by State Grid Corporation of China (SGCC), the UHVDC system has a voltage of 800kV and a capacity of 7.2GW. The project was approved in April 2007

and commissioned in July 2010. The electricity supplied by the transmission line is sufficient to meet the needs of 24 million people. The UHVDC technology used by the transmission line enables direct current (DC) electricity to be transmitted at high voltages and at an efficient rate that prevents losses up to (0.7%) of the rated power. The technology also helps in saving 1.2 million tonnes of carbon emissions from the project due to low energy wastage.

- The Changji-Guquan ultra-high-voltage direct current (UHVDC) transmission line in China is the world's first transmission line operating at 1,100kV voltage. Owned and operated by state-owned State Grid Corporation of China, the 1,100kV DC transmission line also covers the world's longest transmission distance and has the biggest transmission capacity globally. The transmission line traverses for a total distance of 3,324km and is capable of transmitting up to 12GW of electricity. Construction on the £4.7bn ($ 5.9bn) transmission project was started in January 2016 and completed in December 2018.

- The Belo Monte-Rio de Janeiro ultra-high-voltage direct current (UHVDC) transmission line in Brazil, also known as the Belo Monte UHVDC Bipole II line, is the world's longest 800kV power transmission line. The 2,539km-long transmission project is owned and operated by Xingu Rio Transmissora de Energia (XRTE), a subsidiary of Chinese state-owned State Grid Corporation of China (SGCC). The Belo Monte-Rio de Janeiro line is the second UHVDC transmission line to be built for drawing power from the 11.2GW Belo Monte hydroelectric power plant.in northern Brazil to the sub-stations in south-east Brazil. Construction on the £1.85bn ($2.14bn) project was started in September 2017 and completed in March 2019.

- The Zhangbei high-voltage direct current (HVDC) power transmission project in China is the world's first HVDC power transmission system to utilise multi-level voltage sourced converter (VSC) technology at a rated voltage of ±500kV. Owned and operated by State Grid Corporation of China (SGCC), it is an advanced VSC-HVDC system with four interconnected converter stations in a ring network, designed to transmit up to 4,5GW of clean energy. The construction on the £1.4bn ($1.84bn) project was officially commenced in February 2018 following the approval of the National Development and Reform Commission in December 2017. A test run was successfully conducted to energise the four-terminal ring grid by interconnecting the Zhangbei, Kangbao, Fengning, and Beijing converter stations for the first time in June 2020 [16].

Chapter 2

High-Voltage Direct Current Transmission

2.1 Introduction

This chapter discusses the fundamentals of HVDC transmission. There are two major HVDC transmission systems described: line-commutated current-source converters and forced-commutated voltage-source converters.

2.2 HVDC Converter Arrangements

For optimal performance, HVDC converter bridges and cables can be stacked in a variety of designs [17]. As shown in Fig. 2.1, converter bridges can be either monopolar or bipolar.

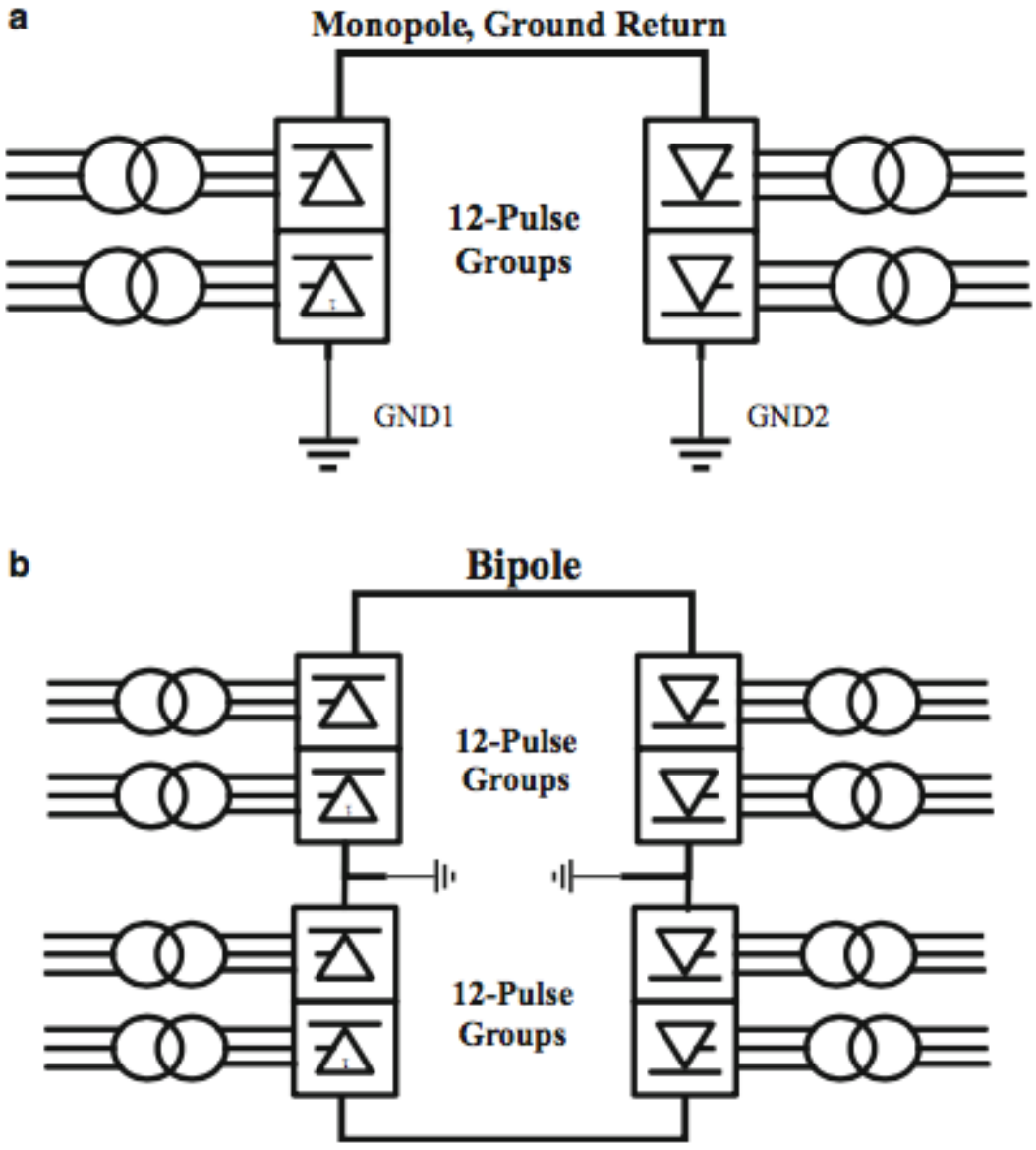

Figure 2.1: Monopolar (a) and bipolar (b) connection of HVDC converter bridges

Fig 2.1.(a) shows a monopolar HVDC system. Two converters are used in this setup, separated by a single pole line, and a positive or negative DC voltage is employed [18]. The following are the main characteristics of a monopolar HVDC system:

- Single high-voltage conductor.
- Current return through the ground.
- OMany existing subsea cable transmissions use monopolar system.

Fig. 2.1.(b) shows a bipolar HVDC system. This is the most popular HVDC system arrangement in applications that employ overhead lines to carry power. The bipolar system, in reality, is made up of two monopolar systems [6]. Fig. 2.1.(b) shows the bipolar current source converter (CSC) setup. The following are the main characteristics of a bipolar HVDC system:

- Two conductors, positive and negative polarity.
- Midpoint connected to the ground.
- The connection between the two sets of converters is grounded either at one or at both ends.
- One of the poles can continue to transmit power in case the other one is out of service.

Multiterminal HVDC system: As in the bipolar case, there are more than two sets of converters in the design shown in Fig. 2.2. As a result, converters one and three can function as rectifiers, while converter two can function as an inverter. Converter two can be used as a rectifier, while converters one and three can be used as inverters if they are used in the reverse sequence [19, 20]. Back-to-back HVDC system: In Fig.2.3, the two converter stations are on the same site, hence no transmission line or cable is needed between the converter bridges. It's possible that the link is monopolar or bipolar. The rated frequency of the two interconnected AC systems may be the same or different, i.e. 50 Hz or 60 Hz. This kind of connecting can also be employed to keep the AC system stable. The back-to-back converter consists of a rectifier and an inverter connected with a common DC link. TThe following are the properties of this combination [20]:

- The DC-link voltage must be higher than the peak line operating voltage.
- The DC-link voltage is regulated by controlling the power flow to the AC grid.
- The possibility of fast control of the power flow.

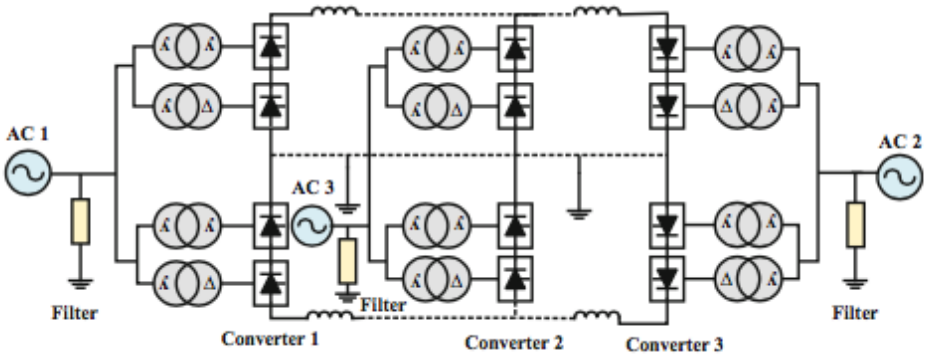

Figure 2.2: Multiterminal HVDC system.

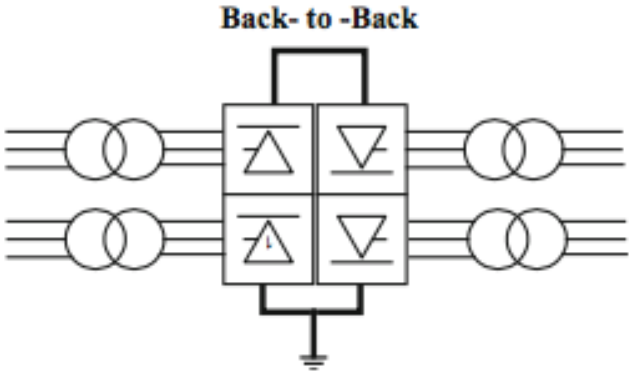

Figure 2.3: Back-to-back converter system.

2.3 Classic HVDC Transmissions

A classic HVDC system in Fig. 2.4 consists of AC filters or other reactive compensation equipment, converter transformers, converters, DC reactors, DC filters, and DC lines or cables [21, 22]. A thyristor is the most common valve type in classical HVDC converters. Thyristors may conduct huge currents in the kilo-amp range and can also block high voltages [23]. As the basic converter unit of conventional HVDC, the 6-pulse bridge of Fig. 2.4 can be employed as both a rectifier and an inverter. Two 6-pulse converter bridges can be connected in parallel or in series to make a 12-pulse converter bridge. Each bridge is made up of a specific number of series-connected thyristors. Converter transformers, one with a YY winding structure and the other with a Y-winding construction, link the bridges to the AC system separately. In this way, the fifth and seventh harmonic currents through the two transformers are in opposite phase that helps to reduce the distortion in the ac system [24]. The HVDC converters are the most important component of an HVDC system. On the rectifier side, they convert AC to DC, and on the inverter side, they convert DC to AC. By using converter transformers, HVDC converters are connected to the AC system. CSCs are utilized in classical HVDC transmission, as previously stated. CSC serves as a constant voltage source on the AC side of the converter. It necessitates the use

of a capacitor as an energy storage device, massive AC filters to eliminate harmonics, and a reactive power supply to rectify power factor. CSC serves as a continuous current source on the DC side of the converter. CSC requires an inductor as its energy storage device in this situation, as well as DC filters with adequate fault current-limiting capabilities. CSC has a number of advantages, the most important of which is its minimal switching losses.

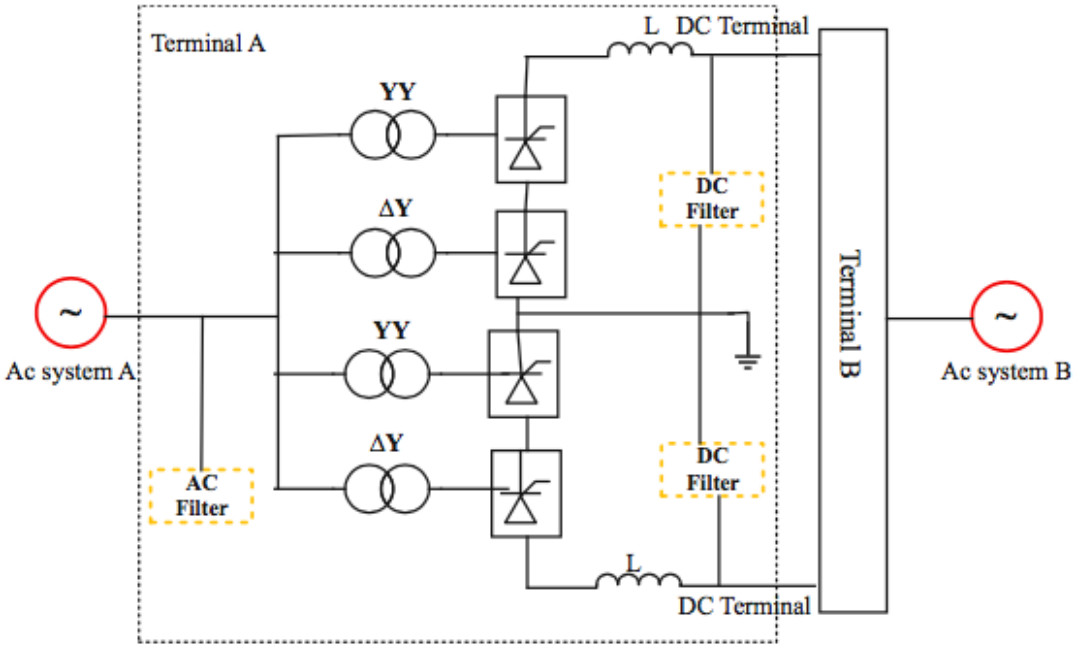

Figure 2.4: A basic configuration for a classic HVDC system

2.4 Main structure of a VSC-HVDC transmission system

2.4.1 VSC-Based HVDC System

Self-commutating switches, such as gate turn-off thyristors (GTOs) or insulated gate bipolar transistors (IGBTs), are used in VSCs and can be controlled to turn on or off. VSCs use the (PWM) technology to function at a high switching frequency of 10 kHz. When compared to traditional thyristor-based HVDC [25], the novel transmission method has the following advantages:

- Possibility to control the reactive power independent of the active power (to or from the converter) without any needs for extra compensating equipment.
- Little risk of commutation failures in the converter.
- Possibility to connect the VSC-HVDC system to a "weak" AC grid or even to one where no generation source is available and naturally the short-circuit level is very low [18].

- OFaster dynamic response due to higher switching frequency operation (phase-controlled), which further results in reduced need for filtering and hence smaller filter size [19].
- Minimal environmental impact.

However, compared to traditional HVDC transmission, VSC transmission has certain disadvantages, including potentially substantial switching power losses and high capital costs, while the technology is still evolving (Table 2.1).

Function	Classic HVDC	VSC- HVDC
Converter valves	Thyristor	IGBT
Connection valve-AC grid	Converter transformer	Series reactor (+ transformer)
Filtering and reactive compensation	50 per in filters and shunt capacitors	Only small filter
DC current smoothing	Smoothing reactor + DC filter	DC capacitor
Telecom between converter station controls	Needed	Not needed

Table 2.1: Comparison of classic and VSC-HVDC systems .

2.4.2 Components of a VSC-HVDC station

The complete description of a VSC-HVDC transmission system is presented in Fig. 2.5. Apart from the switching valves, the station is comprised of a number of other key components as well, that are necessary for the proper operation of the converter.

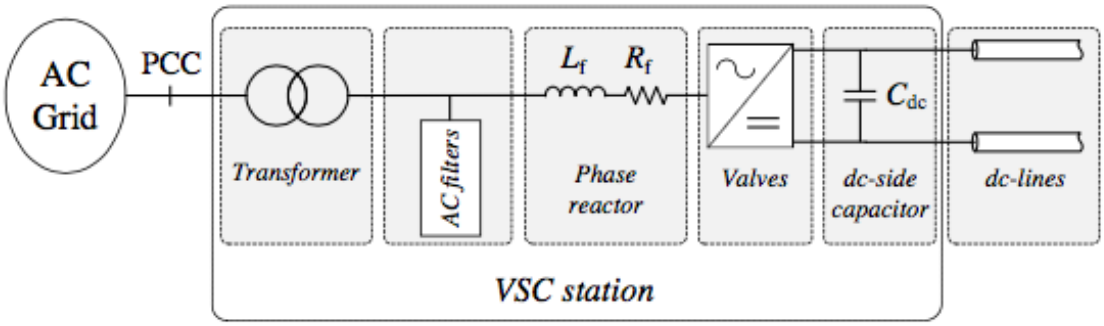

Figure 2.5: Components of a VSC-HVDC station.

AC-side transformer

A VSC station is usually connected to the ac grid via a converter transformer. Its main function is to facilitate the connection of the converter to an ac system whose voltage has a

different rated value. Furthermore, the transformer blocks the propagation of homopolar harmonics to the main ac system, while at the same time provides galvanic isolation between the latter and the VSC station.

Phase reactor

The phase reactor is one of the key components of a VSC station. Its main function is to fa- cilitate the active and reactive power transfer between the station and the rest of the ac system. With the one side of the reactor connected to the ac system, the VSC is able to apply a fully controlled voltage to the other side of the reactor. The magnitude and phase difference of the latter, compared to the ac-system voltage will induce a controlled amount of active and reactive power transfer over the reactor. A secondary function of the phase reactor is to filter higher harmonic components from the converter's output current and also limit short-circuit currents through the valves.

AC-side filters

The voltage output of the HVDC converters is not purely sinusoidal but contains a certain amount of harmonics, due to the valve switching process. This causes the current in the phase reactor to also contain harmonics at the same frequencies, apart from the desired sinusoidal component at the grid frequency. Aiming to reduce the harmonic content of the VSC voltage output, a range of passive filters are used, connected in shunt between the phase reactor and the transformer [2, 44]. Typical examples are 2nd order filters, 3rd order filters or notch filters, as depicted in Fig. 2.6. Depending on the converter topology and its switching levels, the harmonic content of the converter output can be reduced to a level where the necessary ac-side filters can be reduced in number and size or even neglected.

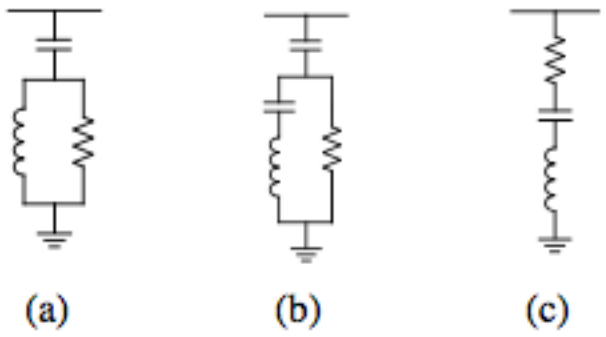

Figure 2.6: AC-side filters. (a) 2nd order filter, (b) 3rd order filter and (c) Notch filter.

DC-side capacitor

The main function of the dc-side capacitor is to reduce the voltage ripple on the dc-side and provide a sufficiently stable direct-voltage from which alternating voltage will

be generated on the ac-side of the converter. Furthermore, the capacitor acts as a sink for undesired high- frequency current components that are generated by the switching action of the converter and are injected to the dc-side. Additionally, the dc-side capacitor acts as a temporary energy storage where the converters can momentarily store or absorb energy, keeping the power balance during transients. The capacitor is characterized by the capacitor time constant, defined as:

$$\tau = \frac{C_{\mathrm{dc}} v_{\mathrm{dc,N}}^2}{2 \cdot P_{\mathrm{N}}} \tag{2.1}$$

where Cdc is the capacitance, dc,N is the rated pole-to-pole direct voltage and PN is the rated active power of the VSC. The time constant is equal to the time needed to charge the capacitor of capacitance Cdc from zero to dc,N, by providing it with a constant amount of power PN [45]. A time constant of 4 ms is used in [46] and 2 ms in [2].

DC-lines

The transmission of power between VSC-HVDC stations is performed using dc-lines. Each dc- pole is here modeled as a Π-model, with resistance Rpole, inductance Lpole and two identical capacitors with capacitance Cpole/2 each. This is depicted in Fig. 2.7. Transmission lines are normally described in terms of resistance/km/pole r, inductance/ km/pole l and capacitance/km/pole c. With the length of the dc-transmission system being provided in km units, the previous cable elements are defined as:

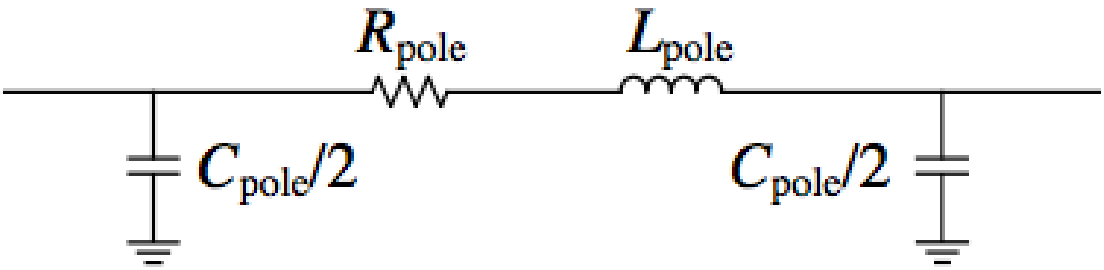

Figure 2.7: Π-model of a single pole for a dc-transmission link.

- $R_{\mathrm{pole}} = r$. (transmission line length).

Type of dc-transmission line	r (Ω/km/pole)	l (mH/km/pole)	c (F/km/pole)
Cable	0.0146	0.158	0.275
Overhead Line	0.0178	1.415	0.0139

Table 2.2: hysical Properties For Modeling DC-Transmission Linesn

- $L_{\mathrm{pole}} = l$. (transmission line length).

- $C_{\text{pole}} = c$. (transmission line length).

It is possible to use two different types of dc-transmission lines: cables or overhead lines. Cable- poles are normally laid very close to each other and therefore have a relatively high capacitance and low inductance per km. On the contrary, overhead transmission line poles are located in a relative distance from each other and as a result they have a relatively high inductance and low capacitance per km. The values that are going to be used in the present thesis are presented in Table 2.2[26].

2.4.3 Converter topologies

The converters so far employed in actual transmission applications are composed of a number of elementary converters, that is, of three-phase, two-level, six-pulse bridges, as shown in Figure 2.8, or three-phase, three-level, 12-pulse bridges, as shown in Figure 2.9.

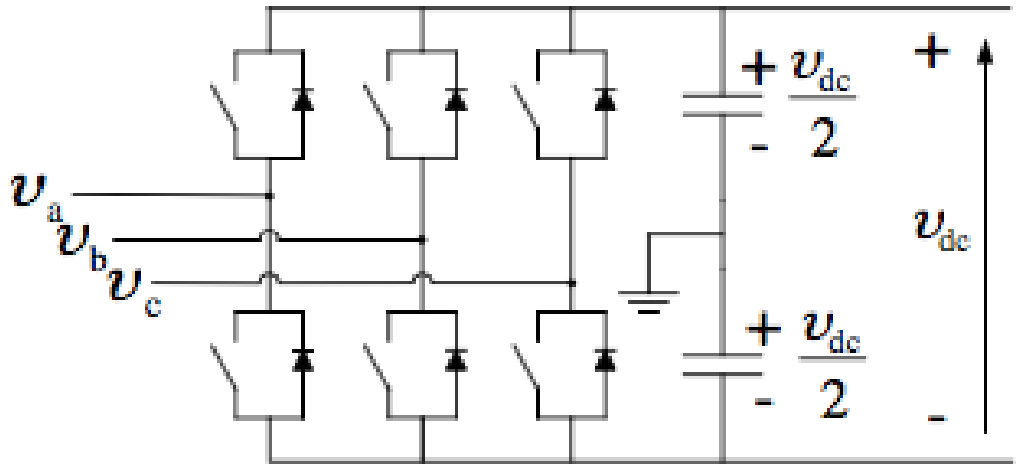

Figure 2.8: Two-level VSC converter.

The two-level bridge is the most simple circuit configuration that can be used for building up a three-phase forced commutated VSC bridge. It has been widely used in many applications at a wide range of power levels. As shown in Fig. 2.8, the two-level converter is capable of generating the two-voltage levels $-0.5 \cdot \text{UdcN}$ and $+0.5 \cdot \text{UdcN}$. The two-level bridge consists of six valves and each valve consists of an IGBT and an anti-parallel diode. In order to use the two-level bridge in high power applications series connection of devices may be necessary and then each valve will be built up of a number of series connected turn-off devices and anti-parallel diodes. The number of devices required is determined by the rated power of the bridge and the power handling capability of the switching devices. With a present technology of IGBTs a voltage rating of 2.5kV has recently become available in the market and soon higher voltages are expected. The

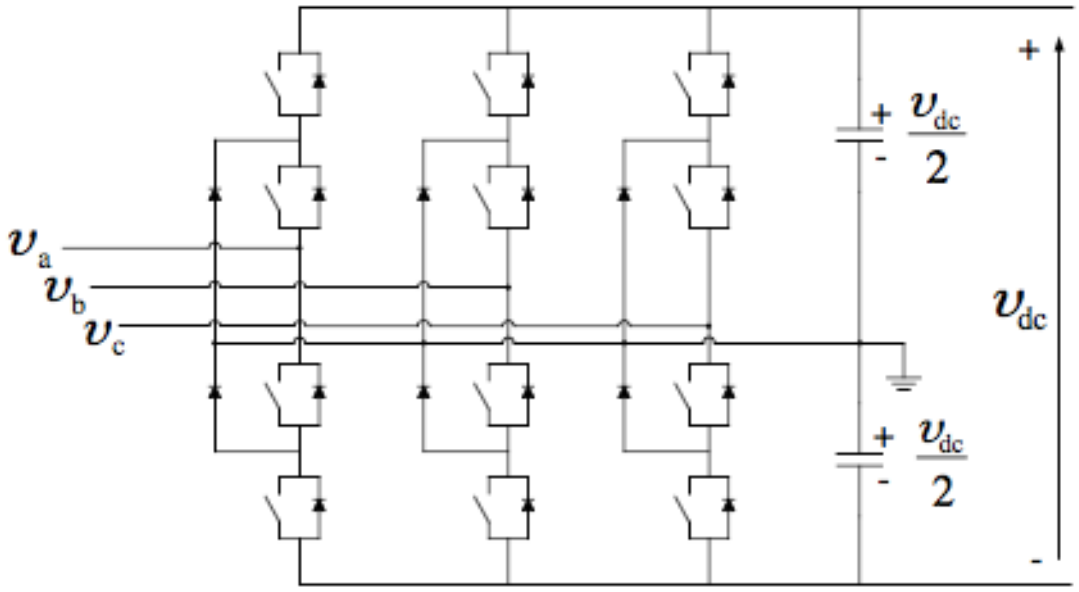

Figure 2.9: Three-level VSC converter.

IGBTs can be switched on and off with a constant frequency of about 2kHz. The IGBT valves can block up to 150kV. A VSC equipped with these valves can carry up to 800A (rms) ac line current. This results in a power rating of approximately 140MVA of one VSC and a ±150kV bipolar transmission system for power ratings up to 200MW[27].

2.5 Operation of VSC-HVDC

The self-commutated PWM technology is used in the VSC-HVDC system. By comparing the instantaneous magnitude of a triangular waveform with a sinusoidal input reference, PWM generates pulse-width modulated signals. Thus, the VSC will generate

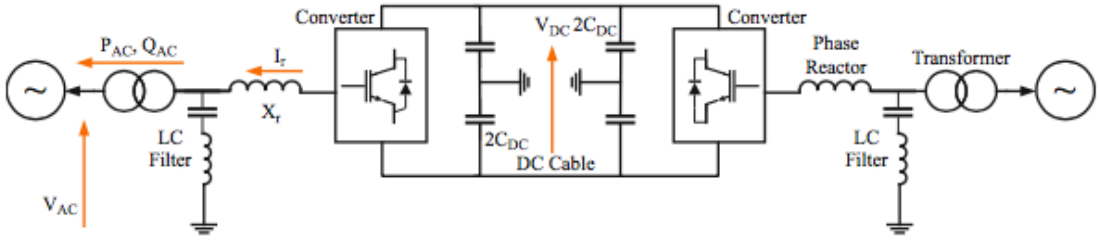

Figure 2.10: Single-line diagram for VSC-HVDC link.

its own voltage waveform without relying on the AC system. PWM regulates the average output voltage over a very short period of time, known as the switching period. The PWM approach generates the required output voltage by using a sinusoidal reference signal. PWM templates, which can be changed practically instantaneously, can be used to manage active and reactive power independently. The power is controlled by changing the fundamental frequency voltage phase angle across the series reactor, whereas the reactive power is controlled by changing the fundamental frequency voltage magnitude across the

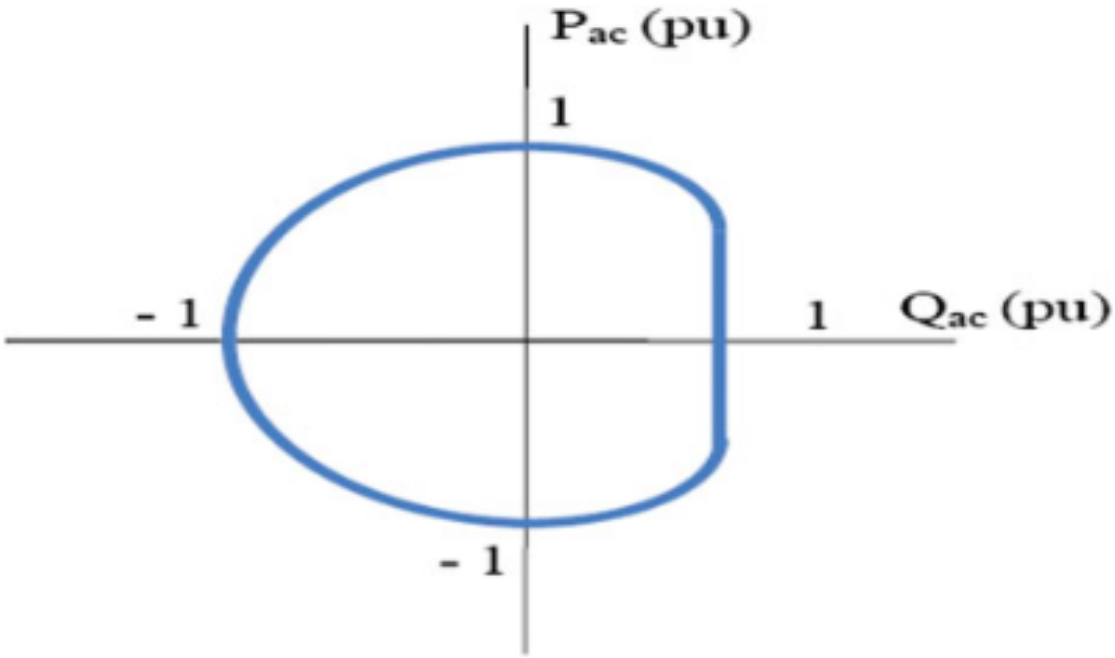

Figure 2.11: Typical P-Q diagram of VSC-HVDC transmission.

series reactor [28]. As shown in Fig. 2.10, two VSC converters are coupled in a back-to-back configuration to establish a transmission link. Each converter can be regulated in all four quadrants of Fig. 2.11 using the PWM technique while maintaining a constant DC voltage. Reactive power on each terminal can be adjusted by adjusting AC voltage, regardless of the converters' transmission power or voltage rating [29].

2.6 Difference from Classical HVDC and Advantages

The fundamental difference in operation between classical HVDC and VSC-HVDC is the latter's greater controllability. As a result, there are a variety of new benefits and uses, some of which are listed below [30]:

- Classic HVDC terminals can provide limited control of reactive power by means of switching of filters and shunt banks and to some level by firing angle control. However, this control requires additional equipment and therefore extra cost. With PWM, VSC-HVDC offers the possibility to control both active and reactive power independently. Hence, independent control of active and reactive power is possible without any needs for extra compensating equipment.

- The reactive power capabilities of VSC-HVDC can be used to control the AC network voltages and thereby contribute to an enhanced power quality. Furthermore, the faster response due to increased switching frequency (PWM) offers new levels of performance regarding power quality control such as flicker and mitigation of voltage dips, harmonics, etc.

- HVDC light does not rely on the AC network's ability to keep the voltage and frequency stable. Independence of AC network makes it less sensitive for disturbances in the AC network, and AC faults do not drastically affect the DC side. If AC systems have ground faults or short circuits, whereupon the AC voltage drops, the DC power transmitted is automatically reduced to a predetermined value. Hence, there is no contribution to the short-circuit currents.
- By controlling grid voltage level, VSC can reduce losses in the connected grid.
- Disturbances in the AC system may lead to commutation failures in classic HVDC system. As VSC-HVDC uses self-commutating semiconductor devices, the risk of commutation failures is significantly reduced.
- The control systems on rectifier and inverter side operate independently of each other. They do not depend on a telecommunication connection. This improves the speed and the reliability of the controller.
- The VSC converter is able to create its own AC voltage at any predetermined frequency, without the need for rotating machines. HVDC Light can feed load into a passive network.
- VSC converters are very suitable for creating a DC grid with a large number of converters, since very little coordination is needed between the interconnected VSCs.
- Transient over voltages can be counteracted by fast reactive power response. Thus, stability margins are enhanced because of reactive power support. More- over, the grid can be operated closer to upper limit, and higher voltage level allows more power transfer.
- Unlike conventional HVDC converters, VSC can operate at very low power. As the active and reactive powers are controlled independently, even at zero active power, the full range of reactive power can be utilized. Active power transfer can be quickly reversed without any change of control mode and without any filter switching or converter blocking. The power reversal is obtained by changing the direction of the DC current and not by changing the DC voltage as for conventional HVDC.

2.7 Conclusion

This chapter serves as an introduction to the concept of the VSC technology and focuses on its application to HVDC transmission systems. The main parts of a VSC-HVDC station have been presented, followed by the presentation of already available or futuristic VSCs that can be used in a station.

Chapter 3

VSC-HVDC Control System

3.1 Introduction

The converters and their control strategies play an important role in converting, transmitting and improving the performance of a high voltage direct current (HVDC) system. Different converter types and control strategies are employed in the HVDC system, such as line commutated converter, voltage source converter (VSC), etc. In VSC-based HVDC transmission systems, the transfer of power is controlled in the same way as in a classic HVDC transmission. The inverter side controls the active power, while the rectifier side controls the DC Voltage but contradicts classic HVDC. VSC-HVDC makes it possible to control the reactive power and the active power independently.Figure 3.1 represents the control structure of the VSC-HVDC transmission system.

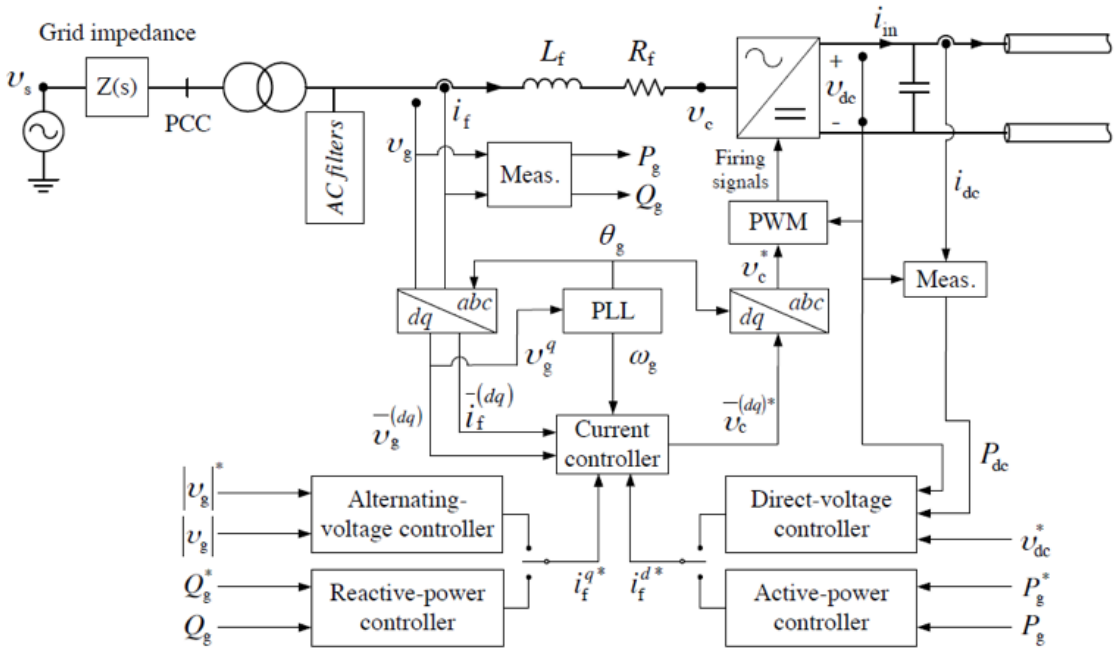

Figure 3.1: VSC control system.

3.2 VSC Converter Control Principles

A controller for VSC should fulfil the following goals:

- Regulation of system variables of importance - Commonly, some of the following variables are regulated at reference values:
  - DC voltage, to ensure lowest losses and to prevent insulation damage;
  - power transfer in accordance with schedule requirements;
  - Reactive power exchange;
  - AC voltage level – this control may be of importance with very weak (high impedance) AC grids.

- Protect the converter from damage caused by currents or voltages that are higher than the rated values.
- Ensure that the system is stable and responds quickly. This necessitates bounded responses and good transient performance of system variables under all anticipated operating conditions and disturbances.
- Support for the local AC grid. With low-inertia AC grids, the VSC is typically necessary to achieve frequency stability via frequency droop feedback. Voltage stabilisation may be necessary in high-impedance systems.

The above control functions are frequently achieved with two-level cascaded converter control where the inner control assures protection and stability whereas the outer control achieves regulation/performance goals. The inner loops generally use fast decoupled current control. The outer control achieves various regulation and stabilisation functions by sending references for the inner current control loops.[31]

3.3 Control Strategies

The efficacy of grid interfaced VSC based HVDC system depends on the control strategy. The designs of this controller coupled with the correct selection of its parameters will have a considerable impact on the system stability. In the controller structure, each control loop has its own control rule and parameters.

For the control of VSC-HVDC, different control strategies have been established in the literature. The very basic of VSC-HVDC control is the voltage controller method, it uses voltage control scheme. In addition, it has direct control of the reactive power controller and power angle controller. In this scheme, the phase-angle shift controls the active power between VSC and the AC system. Power angle is obtained from terminal voltage and current value. The desired power angle achieves an error which will be processed by the angle controller to become reference phase angle. The VSC voltage magnitude controls the reactive power. The reactive power also depends on the modulation index. The actual value of reactive power is called the reference reactive power which obtains an error. This error will be processed by the reactive powercontroller to become the magnitude of the modulating signal. Phase Locked Loop (PLL) will synchronize the output voltage of the inverter to the grid [32]–[33]. This is a straightforward and uncomplicated procedure to be employed. However, the outcome from both reactive power controllers and power angle controllers show that both active and reactive power is the function of power angle which means active power and reactive power cannot be controlled independently [34]. Specifically, the control bandwidth of power angle controller is constrained by the grid frequency and a resonant peak and it cannot limit the current flowing into the converter, thus issuing problems to the system if the over current fault occurs. Due to these disadvantages, the use of this type of control is not very common. [35]

The dominant method in the control of VSC in various applications is the Vector current controller method (VCC) also called the vector control method . This method is designed to overcome the problem encountered by the voltage controller that cannot

control active and reactive power independently. It entails converting from a three-phase steady state to the d-q axis in order to control active and reactive power separately. Vector theory is most widely used in the control of three-phase PWM converters these days.

No.	Control method	Operation	Advantages	Disadvantages
1	Voltage Controller .	.Direct control over active power, reactive power and power angle.	.Simple and easy process.	.Active power and reactive power cannot be controlled independently. .Cannot limit the current flowing into the converter.
2	Vector Current Controller.	.Steady state operation into the d-q axis to control active power and reactive power separately.	.Fast dynamic response. .Delivers better power quality during harmonics and grid disturbances. .Can compensate grid harmonics.	.Achieves poor performance when it is applied to DC link connected to weak AC network.
3	Advanced Vector Current Controller.	.Outer loop control including four decoupling gains to incorporate parameter-varying scheme and overcome system non-linearity.	.Better handle capability to interact with weak or very weak AC grid.	.Ignores the asymmetrical fault and any sudden change during grid operation.
4	Power Synchronization.	.Uses a phase angle to control active power, and voltage value to control reactive power, .Does not use PLL to control the power synchronization.	.Eliminates the possible instability caused by PLL when connected to a weak AC system. .Does not need to have a pre-set current value and does not depend on an inner current loop.	.Over current on the converter valves during the severe AC system fault occurrence. .High load angles when it is interconnected to a weak AC system.
5	ABC Frame Controller.	.VSC is regulated in ABC frame without PLL operation. .The active power and reactive power are controlled exclusively at the point of coupling (PCC).	.Achieves good synchronization when VSC-HVDC connected to weak AC network. .Fast output of reference current. .Feedback currents delay and adaptive filter are not required in the grid voltage frequency variation and harmonic distortion.	Complex structure and operation to control active and reactive power.
6	Voltage Droop Control.	.Selects the droop parameters based on the steady-state analysis. Inner loop controls current while an outer loop regulates DC voltage.	.Reduce the effect of DC voltage disturbances.	.Reference current control could diverge in any sudden change during grid operation.
7	Adaptive Back Stepping Controller.	.Uses DC cable dynamics to maintain DC bus voltage at a rated value and DC voltage at constant value.	.Reduce the overshoot voltage in both wind farm and grid side terminals, thus, the performance of existing DC voltage controller has been improved.	.Does not take into account the model uncertainties which could affect the overall system performance.

Figure 3.2: COMPARATIVE ANALYSIS OF VARIOUS CONTROL STRATEGIES.

There are several control strategies The table above shows a comparative analysis of various control strategies.

3.4 Three-level Pulse Width Modulation Technique

The principle of the pulse width modulation (PWM) technique; a high-frequency triangular carrier wave is compared with a sinusoidal control signal at the desired frequency. The intersection of the control signal and the triangular carrier waves determines the switching instants and commutation of the modulated pulse. A transition in PWM waveform is generated at each compare match point. When sinusoidal wave has magnitude higher than the triangular wave the PWM output is positive and when the control signal is smaller than the triangular carrier wave, the output is negative.

3.5 Vector Control Principle

The backbone of VSC-HVDC control system is the current control. This control structure receives as inputs the currents references i_f^{d*} and i_f^{q*}, having a role of creating a pair of voltage reference v_c^{d*} and v_c^{q*}. These are transformed into three-phase quantities and provided as modulating signals to the PWM block, which will generate appropriate firing signals for the VSC valves. The modulating voltage signal to the PWM is internally normalized by the value of the direct voltage of the dc-side capacitor in the VSC . A Phase-Locked Loop (PLL) is used to synchronize the dq-rotating frame of the converter to the rotating vector $v_g^{(\alpha\beta)}$ in $\alpha\beta$-coordinates, providing a reliable reference frame for any abc-to-dq and dq-to-abc transformations. A number of outer controllers are implemented in order to control other quantities such as the direct voltage of the dc-side capacitor, the active and reactive power transfer, and the magnitude of the alternating voltage v_g. In the VSC station, the desired active and reactive power exchange is imposed at the phase reactor connection point, which connects the VSC main valves to the transformer, as shown in Fig. 3.1. This is the power entering the phase reactor in a positive direction, corresponding to P_g and Q_g. In the case of a voltage-oriented dq frame, the active-power controller controls the current reference i_f^{d*} . The same applies for the direct-voltage controller because the energy stored in the dc-side capacitor (and therefore its voltage) is controlled by active power injected to it by the VSC. As a result, the reference i_f^{d*} can be utilized for either active-power or direct-current control. The reactive power is controlled by i_f^{q*} , and since the magnitude of the alternating voltage v_g is related to the amount of reactive-power transfer by the VSC, the reference i_f^{q*} is utilized either for reactive power or alternating voltage control. [26]

In this chapter, the several control blocks that form the whole VSC control system are individually presented. Observe that the use of boldface in expressions denotes complex space vectors, whereas the overline notation "(overline)" denotes a real space vector.

3.5.1 Inner Current Controller

The Inner Current Controller, which will be referred to simply as Current Control (CC) from now on, is at the heart of the VSC-control scheme. Considering the equivalent process representing the VSC in Fig.3.3, if Kirchhoff's voltage law (KVL) is applied across the phase reactor, the following combined description of differential equations can be obtained for the three phases

$$v_{\mathrm{g}}^{(abc)} - v_{\mathrm{c}}^{(abc)} = L_{\mathrm{f}} \frac{di_{\mathrm{f}}^{(abc)}}{dt} + R_i i_{\mathrm{f}}^{(abc)} \tag{3.1}$$

By applying Clarke's transformation (described in the Appendix), (3.1) can be expressed in the fixed $\alpha\beta$-coordinate system as :

$$\bar{v}_{\mathrm{g}}^{(\alpha\beta)} - \bar{v}_{\mathrm{c}}^{(\alpha\beta)} = L_f \frac{di_{\mathrm{f}}^{(\alpha\beta)}}{dt} + R_{\mathrm{f}} \iota_{\mathrm{f}}^{(\alpha\beta)} \tag{3.2}$$

A further step is to apply the Park transformation (see Appendix). The PLL of the VSC is synchronized with the voltage vector $\bar{v}_{\mathrm{g}}^{(dq)}$. The considered voltage and current vectors can then be expressed as:

$$\begin{aligned} \bar{v}_{\mathrm{g}}^{(\alpha\beta)} &= \bar{v}_{\mathrm{g}}^{(dq)} e^{j\theta_{\mathrm{g}}} \\ \bar{v}_{\mathrm{c}}^{(\alpha\beta)} &= \bar{v}_{\mathrm{c}}^{(dq)} e^{j\theta_{\mathrm{g}}} \\ \bar{i}_{\mathrm{f}}^{(\alpha\beta)} &= \bar{l}_{\mathrm{f}}^{(dq)} e^{j\theta_{\mathrm{g}}} \end{aligned} \tag{3.3}$$

Equation (3.2) can thus be transformed into:

$$\begin{aligned} &\bar{v}_g^{(dq)} e^{j\theta_g} - \bar{v}_{\mathrm{c}}^{(dq)} e^{j\theta_g} = L_{\mathrm{f}} \frac{d\left(\bar{i}_f^{(\mathrm{dq})} e^{j\theta_{\mathrm{g}}}\right)}{dt} + R_{\mathrm{f}} \bar{i}_f^{(dq)} e^{j\theta_g} \Rightarrow \\ &\bar{v}_{\mathrm{g}}^{(dq)} e^{j\theta_{\mathrm{g}}} - \bar{v}_{\mathrm{c}}^{(dq)} e^{j\theta_{\mathrm{g}}} = j \frac{d\theta_{\mathrm{g}}}{dt} L_{\mathrm{f}} \bar{i}_{\mathrm{f}}^{(dq)} e^{j\theta_{\mathrm{g}}} + L_{\mathrm{f}} e^{j\theta_{\mathrm{g}}} \frac{d\bar{i}_{\mathrm{f}}^{(dq)}}{dt} + R_{\mathrm{f}} \bar{i}_{\mathrm{f}}^{(dq)} e^{j\theta_{\mathrm{g}}} \Rightarrow \\ &\bar{v}_{\mathrm{g}}^{(dq)} e^{j\theta_{\mathrm{g}}} - \bar{v}_{\mathrm{c}}^{(dq)} e^{j\theta_{\mathrm{g}}} = j_{\mathrm{g}} L_{\mathrm{f}} \bar{i}_{\mathrm{f}}^{(dq)} e^{j\theta_{\mathrm{g}}} + L_{\mathrm{f}} e^{j\theta_{\mathrm{g}}} \frac{d\bar{i}_{\mathrm{f}}^{(dq)}}{dt} + R_{\mathrm{f}} \bar{i}_{\mathrm{f}}^{(dq)} e^{j\theta_{\mathrm{g}}} \end{aligned} \tag{3.4}$$

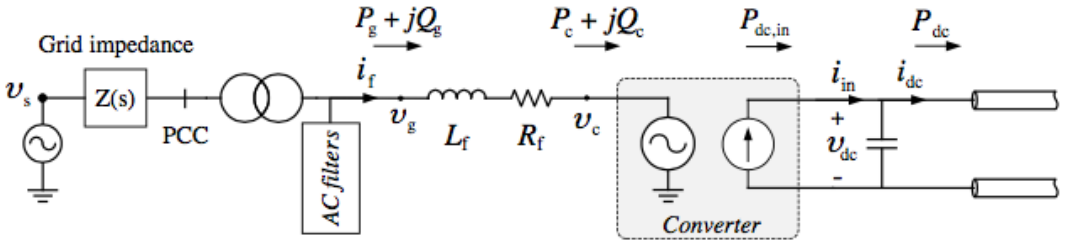

Figure 3.3: Equivalent model of the VSC.

where w_g is the angular frequency of the dq-rotating frame. Usually, the variations in $w_g(t)$ are very small over time and $w_g(t)$ can then be replaced by a constant value of w_g. Under this condition and eliminating the term $e^{j\theta_{\mathrm{g}}}$, (3.4) can be re-written as:

$$L_{\mathrm{f}} \frac{d\bar{i}_{\mathrm{f}}^{(\mathrm{dq})}}{dt} = -R_{\mathrm{f}} \bar{i}_{\mathrm{f}}^{(dq)} - j_{\mathrm{g}} L_{\mathrm{f}} \bar{i}_{\mathrm{f}}^{(dq)} + \bar{v}_{\mathrm{g}}^{(dq)} - \bar{v}_{\mathrm{c}}^{(dq)} \tag{3.5}$$

which can be expanded to its real and imaginary part as:

$$L_{\mathrm{f}}\frac{di_{\mathrm{f}}^{d}}{dt} = -R_{\mathrm{f}}\overset{d}{\mathrm{f}} +_{\mathrm{g}} L_{\mathrm{f}} i_{\mathrm{f}}^{q} + v_{\mathrm{g}}^{d} - v_{\mathrm{c}}^{d} \tag{3.6}$$

$$L_{\mathrm{f}}\frac{di_{\mathrm{f}}^{q}}{dt} = -R_{\mathrm{f}} i_{\mathrm{f}}^{q} -_{\mathrm{g}} L_{\mathrm{f}} i_{\mathrm{f}}^{d} + v_{\mathrm{g}}^{q} - v_{\mathrm{c}}^{q} \tag{3.7}$$

These are two cross-coupled first-order subsystems, with the cross-coupling being initiated by the terms $w_g L_f i_f^q$ and $w_g L_f i_f^d$.

The complex power S_g can be decomposed into the active and reactive power as follows

$$S_{\mathrm{g}} = \bar{v}_{\mathrm{g}}^{(dq)} \left[\bar{i}_{\mathrm{f}}^{(dq)}\right]' = \left(v_{\mathrm{g}}^{d} + j v_{\mathrm{g}}^{q}\right)\left(i_{\mathrm{f}}^{d} - j i_{\mathrm{f}}^{q}\right) \Rightarrow S_{\mathrm{g}} = \left(v_{\mathrm{g}}^{d} i_{\mathrm{f}}^{d} + v_{\mathrm{g}}^{q} i_{\mathrm{f}}^{q}\right) + j\left(v_{\mathrm{g}}^{q} i_{\mathrm{f}}^{d} - v_{\mathrm{g}}^{d} i_{\mathrm{f}}^{q}\right) \Rightarrow$$

$$P_{\mathrm{g}} = v_{\mathrm{g}}^{d} i_{\mathrm{f}}^{d} + v_{\mathrm{g}}^{q} i_{\mathrm{f}}^{q} \tag{3.8}$$

$$Q_{\mathrm{g}} = v_{\mathrm{g}}^{q} i_{\mathrm{f}}^{d} - v_{\mathrm{g}}^{d} i_{\mathrm{f}}^{q} \tag{3.9}$$

Considering that the PLL performs the synchronization by aligning the d-axis of the dq-rotating frame to the vector $\bar{v}_{\mathrm{g}}^{(dq)}$, the q-component of the latter will be zero in steady-state, thus

$$\bar{v}_{\mathrm{g}}^{(dq)} = v_{\mathrm{g}}^{d} \tag{3.10}$$

Applying (3.10) to (3.8) and (3.9) gives

$$P_{\mathrm{g}} = v_{\mathrm{g}}^{d} i_{\mathrm{f}}^{d} \tag{3.11}$$

$$Q_{\mathrm{g}} = -v_{\mathrm{g}}^{d} i_{\mathrm{f}}^{q} \tag{3.12}$$

This indicates that the active power can be controlled via the d component of the current,i_f^d ,while the reactive power with the q component of the current, i_f^q, If the two currents can be controlled independently, the VSC could have an independent and decoupled control of the active and reactive power.

Regarding the active-power balance at the two sides of the valves of the VSC (as reactive power does not propagate to the dc-side) and assuming that the losses on the valves are negligible, the following relation applies:

$$P_{\mathrm{c}} = P_{\mathrm{dc,in}} \Rightarrow \mathrm{Real}\left\{\bar{v}_{\mathrm{c}}^{(dq)}\left[\bar{i}_{\mathrm{f}}^{(dq)}\right]'\right\} = v_{\mathrm{dc}} i_{\mathrm{in}} \Rightarrow v_{\mathrm{c}}^{d} i_{\mathrm{f}}^{d} + v_{\mathrm{c}}^{q} i_{\mathrm{f}}^{q} = v_{\mathrm{dc}} i_{\mathrm{dc}} \Rightarrow$$

$$i_{\mathrm{in}} = \frac{v_{\mathrm{c}}^{d} i_{\mathrm{f}}^{d} + v_{\mathrm{c}}^{q} i_{\mathrm{f}}^{q}}{v_{\mathrm{dc}}} \tag{3.13}$$

As shown in Fig. 3.3, this is the direct current propagating to the dc side of the VSC. In steady-state, the current i_{in} equals i_{dc}, assuming a lossless dc capacitor and neglecting switching harmonics.

Observing (3.4)-(3.6), the only way for the VSC to influence the dynamics of the reactor current and attempt to adjust it to a desired reference $\bar{i}_f^{(dq)*}$ is to change its output voltage $\bar{v}_c^{(dq)*}$. As a result, a control legislation must be used to provide a reference, which the VSC will apply with ideally no delay.

Equation (3.5) can be transformed in the Laplace domain as:

$$sL_f i_f = -R_f i_f - jw_g L_f i_f + v_g - v_c \tag{3.14}$$

where the bold font indicates the Laplace transformation of a corresponding dq-coordinate vector. If the current i_f and the voltage v_g are perfectly measured, the following control law is suggested in [26], which eliminates the cross-coupling of the current dq-components and compensates for the disturbance caused by v_g.

$$v_c^* = -F(s)(i_f^* - i_f) - jw_g L_f + v_g \tag{3.15}$$

where, $F(s)$ is the controller transfer function applied to the current error. If the controller computational delay and the PWM switching are modeled as a delay time T_d, then $v_c = e^{-sT_d} v_c$, [36]. However, for simplification purposes, the delay time can be neglected and then $v_c = v_c^*$. Under this condition and if is equated to a PI controller with proportional $K_{p,cc} = a_{cc} R_f$ gain and integral gain , then substituting (3.14) in (3.13) yields

$$\mathbf{i}_\mathrm{f} = G_\mathrm{cc} \mathbf{i}_\mathrm{f}^\star = \frac{a_\mathrm{cc}}{s + a} \mathbf{i}_\mathrm{f}^\star \tag{3.16}$$

indicating that the closed-loop current control can be shaped as a first-order low-pass filter with bandwidth a_{cc}. The block diagram of the complete CC based on relation (3.14) is presented in Fig. 3.4. Several enhancements to the CC can be made, including :

- anti-windup functionalities in case of voltage saturation;
- active damping capabilities to reject undesired disturbances;
- Signal filtering before they are fed into the control process;

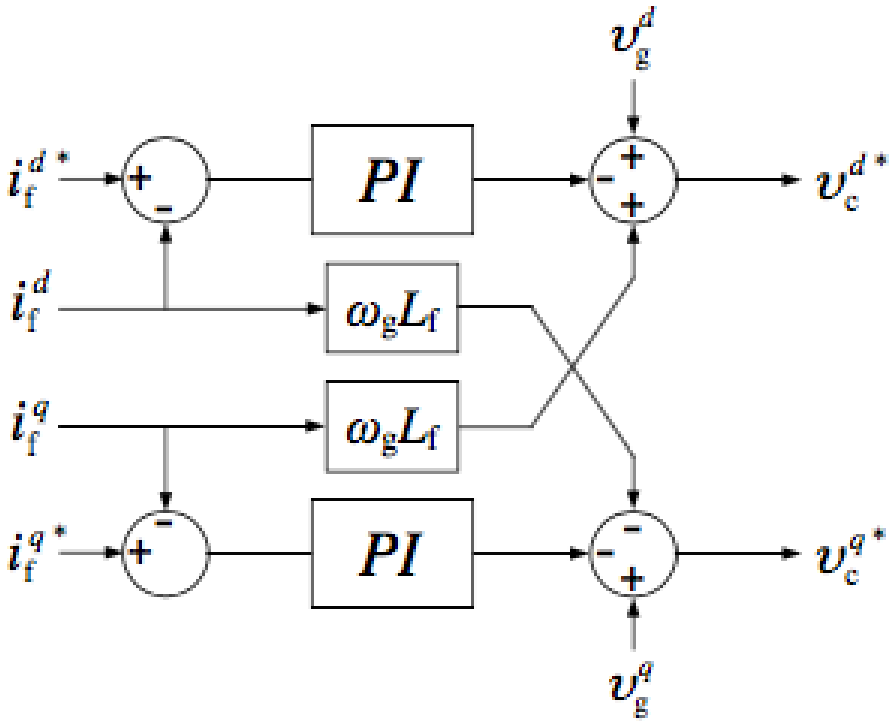

Figure 3.4: Current Controller of the VSC.

3.5.2 Phase-Locked Loop

The fundamental job of a PLL in HVDC systems is to give a reference signal for a converter controller which is synchronised with the AC commutation voltage. As the operating conditions in the AC system change, the zero crossings of AC voltages will move. A thyristor can only be fired when it is forward biased, and in inversion mode it should be fired sufficiently early to allow reverse recovery for given AC voltage magnitudes. Therefore precise information on the AC voltage position is required for converter firing control. The task of the PLL is done in the VSC control structure by determining the angle of rotation θ_g of the measured voltage vector $\bar{v}_g^{(\alpha\beta)}$. Fig. shows $\bar{v}_g^{(\alpha\beta)}$, along with the -stationary frame, the ideally aligned $d_i q_i$ frame (rotating with angular speed w_g and angle θ_g and the converter rotating frame (rotating with angular speed $\widehat{w_g}$ and an angle $\widehat{\theta_g}$). The latter is the frame that is in the knowledge of the PLL, which tries to position it so that the d-axis is aligned with the rotating vector.

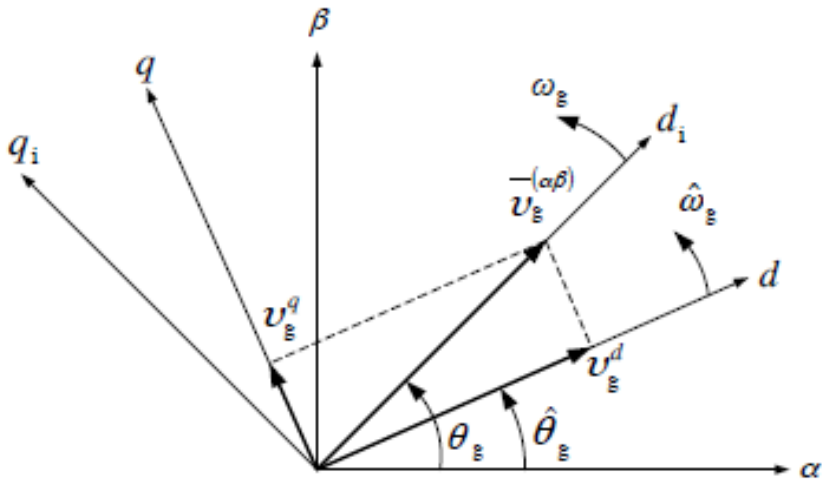

Figure 3.5: Decomposition of the voltage vector $\bar{v}_g^{(\alpha\beta)}$) into the converter dq frame and the ideal dq frame. g.

As it can be seen, as long as the PLL's dq-frame is positioned at $\widehat{\theta_g}$ and is still not properly aligned with $\bar{v}_g^{(\alpha\beta)}$, the dq-decomposition of the vector is going to result in a non-zero q-component v_g^q. The PLL must thus increase or decrease $\widehat{w_g}$ speed (and thus $\widehat{\theta_g}$) until the calculated v_g^q becomes equal to zero. This means that from a control perspective, the term v_g^q can be used as an error signal, which when fed to a PI controller will lead to the creation of such an $\widehat{w_g}$ and $\widehat{\theta_g}$ that eventually will set v_g^q to zero. The structure of the adopted PLL is depicted in Fig. 3.5. The voltage v_g^{abc} is transformed into $\bar{v}_g^{(\alpha\beta)}$ and using the PLL's estimation $\widehat{\theta_g}$, calculates $\bar{v}_g^{(dq)}$. Based on the "error" v_g^q (normalized by $v_{g,0}^d$, the PLL's PI controller outputs a correction signal Δw, which is added to a constant pre-estimation of the vector's angular speed $w_{g,0}$. This provides the converter angular speed $\widehat{w_g}$ and is integrated to produce the updated version of $\widehat{\theta_g}$, which is fed back to the $\alpha\beta$-to-dq block and produces the new v_g^q. In steady-state, $\widehat{w_g}$ and $\widehat{\theta_g}$ become equal to w_g and θ_g, respectively. The gains $K_{p,pll}$ and $K_{i,pll}$ are selected as suggested in [37] as

$$K_{p,pll} = 2a_{pll}, K_{i,pll} = a_{ill}^2 \tag{3.17}$$

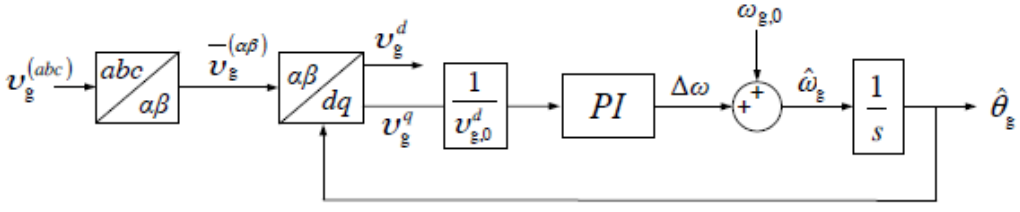

Figure 3.6: Block diagram of PLL.

In [38], a bandwidth a_{pll} for the closed-loop system of 5 Hz is selected and in [39] a

range of 3 to 5 Hz is mentioned as typical bandwidth for grid-connected applications. In this thesis, a_{pll} is selected to be 5 Hz (provided to the controller in rad/s units).

3.5.3 The Outer Controller

Common objectives for the outer loop active power through the converter, reactive power at each side, and DC-link voltage: Active current is used to control active power flow or DC voltage level. Similarly, reactive current is used to control reactive power flow into stiff grid connection. The speed of the outer controller loops is typically selected to be much slower than the inner current controller loop to guarantee stability. For this reason, the current controller can be considered infinitely fast when designing the parameters of the outer controller loops. The outer controllers are typically of proportional integral type in order to ensure satisfactory speed of response and to eliminate tracking error.

- **Direct-Voltage Control**

The portion of the complete VSC model that describes the dynamics of the Direct-Voltage Controller (DVC) is presented in Fig. 3.7. The energy stored in the dc capacitor C_{dc} of the DVC VSC is $C_{dc}W/2$, with the value $W = v_{dc}^2$ being proportional to the energy of that capacitor. The dynamics of the dc capacitor become

$$\frac{1}{2}C_{dc}\frac{\mathrm{d}W}{\mathrm{d}t} = P_{dc,in} - P_{dc} \tag{3.18}$$

The DVC can be a simple PI controller $F(s)$ with proportional gain K_p and integral gain K_i. The output of the controller is a reference P_g^*. Assuming no losses on the phase reactor (neglect R_f) and a lossless converter, we have

$$P_g \approx P_c \approx P_{dc,in} \tag{3.19}$$

Therefore, P_g can be considered as the power that is drawn from the ac grid and directly injected to the dc-side capacitor to keep it charged, as in Fig. From a control point of view, P_{dc} represents a disturbance. Therefore a dc-power feed forward term can be added to cancel its effect in the closed-loop system. Consequently, $F(s)$ can be represented solely by K_p, still maintaining a zero state error under ideal conditions [53]. The incomplete knowledge on the properties of all the converter's components and the unavoidable existence of losses in the system, require K_i to be maintained, providing a trimming action and removing steady-state errors. In the present analysis however, these issues are neglected and $K_i = 0$. The expression of the DVC can then be written as

$$\begin{gathered} P_g^* = F(s)(W^* - W) + P_f = K_p(W^* - W) + P_f \Rightarrow \\ P_g^* = K_p(W^* - W) + H(s)P_{dc} \end{gathered} \tag{3.20}$$

where W^* is the reference "energy" stored in the capacitor, $H(s)$ is the transfer function of a low-pass filter $a_f/(s + a_f)$ having bandwidth a_f, and P_f represents the power-feedforward term of the DVC, equal to the filtered value of P_{dc}. Given (3.11), the

current reference i_f^{d*} could then be equal to $i_f^d = P_g^*/v_g^d$, where v_g^d could optionally be filtered as well through a low-pass filter of bandwidth a_f, as suggested in [53].

Observe that the DVC is not controlling v_{dc} itself but rather the square of the latter, W. If the controller were to operate directly on the error $v_{dc}^* - v_{dc}$, the voltage control process would be non-linear and the small-signal closed-loop dynamics of the system would be dependent on the steady-state operating point $v_{dc,0}$ and, thereby, v_{dc}^* (assuming that v_{dc} normally becomes equal to the reference). This inconvenience is avoided by prompting the controller to alternatively operate on the error $W^* - W$ [53].

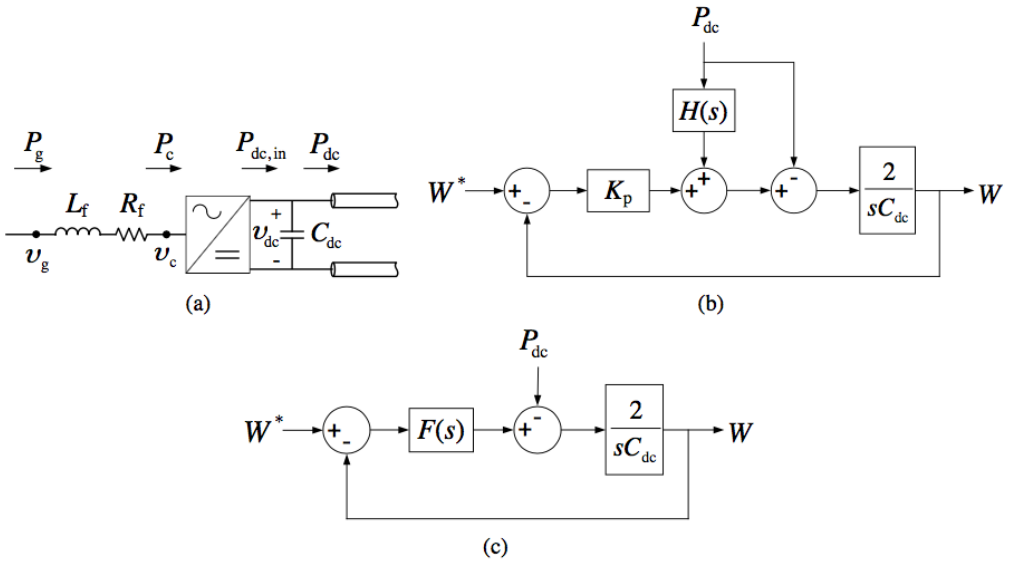

Figure 3.7: Direct-voltage control in a VSC: (a) Power flow across the converter, (b) Closed-loop direct- voltage control process with power feedforward and (c) Closed-loop direct-voltage control process without power feedforward..

Assuming perfect knowledge of the grid-voltage angle and an infinitely fast current-control loop, the requested active power P_g^* can be immediately applied, thus P_g^*=P_g. Substituting (3.20) to (3.18) and considering (3.19), gives:

$$W = \frac{2K_p}{2K_p+sC_{dc}}W^* + \frac{2[H(s)-1]}{2K_p+sC_{dc}}P_{dc} = \frac{\frac{2K_p}{sC_{dc}}}{s+\frac{2K_p}{sC_{dc}}}W^* + \frac{2[H(s)-1]}{2K_p+sC_{dc}}P_{dc} \Rightarrow$$
$$W = G_{cpff}W^* + Y_{cpff}P_{dc} \tag{3.21}$$

where G_{cpff} is the closed-loop transfer function of the direct-voltage control with power feedforward for $P_{dc} = 0$. If the proportional gain is selected as $K_p = a_d C_{dc}/2$, the transfer function G_{cpff} is now equal to $a_d/(s + a_d)$, which is a first-order low-pass filter with bandwidth a_d. This serves as a valuable designing tool for the prediction of the closed-loop performance of the DVC.

It is, however, fairly common practice to use a DVC without a power feedforward term, as in Fig. 3.7(c). In this case, the $F(s)$ must maintain both its proportional and integral gain to guarantee a zero steady-state error, and the closed-loop dynamics become

$$W = \frac{2F(S)}{2F(s)+sC_{dc}} - \frac{2}{2F(s)+sC_{dc}}P_{dc} = G_{cpnff}W^* + Y_{cpnff}P_{dc} \tag{3.22}$$

where G_{cpnff} is the closed-loop transfer function of the direct-voltage control without power feedforward for$P_{dc} = 0$. G_{cpnff} can no longer be equated to a first-order filter but if $K_p = a_d C_{dc}$ and $K_p = a_d^2 C_{dc}/2$ [14], then G_{cpnff} has two real poles at $s = -a_d$.

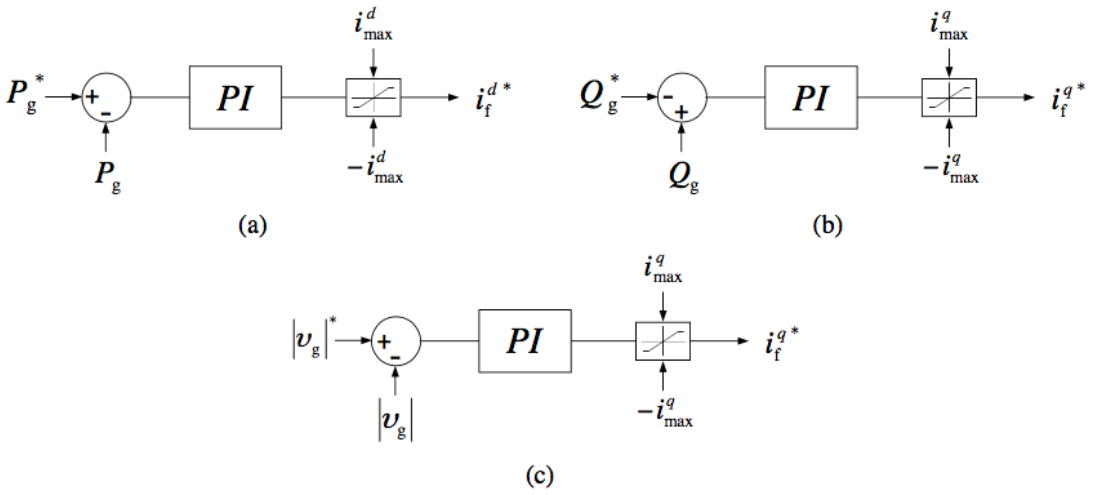

Figure 3.8: (a) Active-Power Controller of the VSC, (b) Reactive-Power Controller of the VSC and (c) Alternating-Voltage Controller of the VSC.

• Active-Power Control

The Active-Power Controller's (APC) function is to set the flow of active power to a certain reference. The connecting point between the phase reactor and the ac-side filters is normally where the active power is measured and controlled in the VSC circuit. If the considered station is in power-control mode, i.e. it is the receiving-end station, the controlled power corresponds to the power P_g that enters the phase reactor towards the valves of the VSC, with regards to Fig. 3.1. As shown in (3.14), the active power depends only on the current i_f^d and v_g^d the voltage. The latter experiences only small variations in practice and its contribution to P_g is considered to be constant. The active power will then be essentially decided by i_f^d. Hence, an active power controller as in Fig. 3.8(a) can be used where a PI controller is engaged to generate the current reference i_f^{d*} that will be supplied to the CC and finally imposed to the phase reactor. The PI typically has a limitation function where the reference i_f^{d*} is limited to a maximum value i_{max}^d equal to a rated propertyi_N. This can be the rated ac current of the converter or a value close to the maximum allowed valve current, both turned into an appropriate *dq*-current quantity.

• Reactive-Power Control

Equation (3.11) shows that the reactive power Q_g that enters the phase reactor is proportion -al to the voltage value v_g^d and the current i_f^d. Consequently, Q_g can be considered solely a function of i_f^d. The PI-based Reactive-Power Controller (RPC) in Fig. can then regulate Q_g to follow a reference Q_g^* by creating an appropriate current i_f^{d*} to be provided to the and finally imposed to the phase reactor. Notice that Q_g and Q_g^* are added with opposite signs than P_g and P_g^* in the previous section, because of the minus sign in (3.11).

The RPC can have a limitation function where the reference i_f^{q*} is limited to a maximum value i_{max}^q. Considering the previous maximum current limitation i_N and a possible strategy that gives priority to the establishment of the separately requested i_{max}^d current, the limit of the reactive current reference can be varied during operation by the relation

$$i_{max}^q = \sqrt{i_N^2 - (i_f^{d*})^2} \tag{3.23}$$

• Alternating-Voltage (AC) Control

The AC voltage control using VSCs may be attractive with very weak grids, i.e.grids with high impedance. The flow of current between such a grid and the VSC would cause significant voltage drop across the grid impedance and drastically change the voltage magnitude at the PCC, and thus the voltage v_g of the phase reactor as in Fig. 3.3. Considering a mostly inductive equivalent impedance of the grid, if the VSC absorbs reactive power, the magnitude of v_g is going to decrease, with the opposite phenomenon occurring for an injection of reactive power from the VSC. Therefore, since the reactive power is regulated through i_f^q, a PI controller can be used as an alternating voltage controller, as in Fig. 3.8(c) . Observe that the signs of adding $|v_g|^*$ and$|v_g|$ are in such a way so that a positive error $|v_g|^*$-$|v_g|$, (demand for increase of voltage magnitude) should cause a demand for negative reactive power and therefore positive i_f^{q*}.

3.6 Issues and Challenges

Despite the fact that VSC has outperformed conventional LCC type converters, there are several shortcomings that need to be addressed. Firstly, grid interaction stability issue such as angle and voltage stability limitations of VSC-HVDC. Secondly, the limitation of the converter like the maximum current and voltage restrictions of the power converter. These limitations need to be considered in designing an efficient controller of VSC-HVDC system. Furthermore, the selection of controller parameters is an important part of controller design since it affects system behavior. Inappropriate parameter selection could lead to system instability. Moreover, there are many problems that could possibly occur when VSC-HVDC is interconnected to a weak AC network.

3.6.1 High Dynamic Overvoltage

When DC power transfer is interrupted, the converter's reactive power absorption falls to zero.Then, the AC voltage will be increased due to the shunt capacitor and harmonic filter. This will necessitate high insulation of system equipment; otherwise, this equipment may be damaged as a result of the overvoltage [35].

3.6.2 Voltage Instability

In this scenario, direct current will be increased in order to restore the system to scheduled power. Consequently, firing angle at inverter will also increase to maintain the commutation margin. Reactive power drawn by the inverter is increased, however reactive power produced by the shunt capacitor is low. This will cause AC voltage to drop yielding towards voltage fall.

3.6.3 Harmonic Resonance

Harmonic resonance might come from parallel resonance at shunt capacitor and harmonic filters, also when the AC system operates at lower harmonics. The conversion process at the converter station becomes more challenging when the need for capacity link increases due to increased short circuit capacity on the commuting bus. Since the converter produces harmonics in current on the AC side and harmonics in voltage on the DC side, harmonics generated by the DC link is also increased when the DC power transmission is increased. On top of that, the interaction between AC and DC in the converter station also generates small amounts of uncharacteristic harmonics even though an equidistant pulse firing scheme is in use. It becomes worse when these uncharacteristic harmonics are injected into poorly damped resonant networks which will make the operating condition of the HV DC/AC system more difficult. If there is a DC side series resonance at the fundamental frequency, the low order harmonic resonance at the AC side might create more severe problems.

3.6.4 Voltage flicker

Voltage variations could occur while switching between the shunt capacitor and reactor, as well as in rapidly changing loads, resulting in AC voltage flicker. Besides, the inter-harmonics is caused by variation in loads that could be the cause of voltage flicker. In fact, handling with inter-harmonics can be more difficult than harmonics. The frequencies in inter-harmonics are not integer multiple of the fundamental frequency, and the magnitude of voltage waveform might fluctuate even in the condition of waveform distortions [35].

3.7 Conclusion

In this chapter, we have presented the control strategies of the VSC-HVDC. The very basic of VSC-HVDC control is voltage controller method, however, the independent control of active and reactive power cannot be achieved with this method. This has been overcome by the VCC method. A range of interlinked controllers that perform the operation of a typical VSC station have been presented, within the general context of vector control. Finally, we listed the issues and challenges of the VSC-HVDC system.

Chapter 4

VSC-HVDC Under DC Fault Conditions

4.1 Introduction

This chapter will look at how high-voltage direct current systems respond to DC faults theoretically. The analysis will include a three-level voltage source converter with an HVDC topology. The test system is depicted in Fig. 4.1, which also shows the location of the flaws. The study is focused on how the system reacts to problems at the DC or AC bus converter.

4.2 Faults on the DC System

Cable faults are more common than system faults [19]. This is owing to the wide range of circumstances that might lead to a DC fault. The most common cause is breakdown or collapse of insulation. However, there are several other reasons that can lead to the same result, such as electrical stresses, environmental conditions, aging, and physical damage. The DC faults that are possible in a HVDC system can be categorized as:

- Positive pole-to-ground fault.
- Negative pole-to-ground fault.
- Pole-to-pole fault.

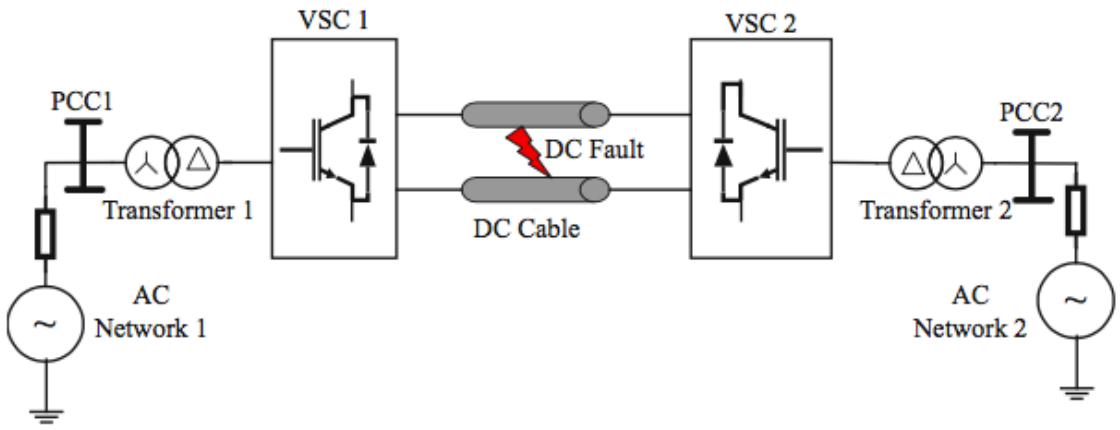

Figure 4.1: A VSC-HVDC transmission system with a location for DC fault.

Because the system is generally symmetrical, the negative pole-to-ground fault can be thought of as a mirror image of the positive pole-to-ground fault. As a result, only the pole-to-pole fault and positive pole-to-ground fault are explored further in the remainder of this thesis. Faults on direct current lines are often pole-to-ground faults [35–49]. A pole-to-pole fault occurs when two active conductors are connected, either directly or via ground. This happens infrequently because it necessitates extensive damage to both HVDC line cables. A short-circuit failure is extremely unusual, especially in undersea cables, where mechanical strains cause the majority of cable problems.

4.2.1 Pole-to-Ground Fault

When one line (either positive or negative pole) is short-circuited to the ground, this type of fault develops. This can happen for a variety of reasons, including those already stated. Most commonly, torn insulation might enable a current passage to ground owing to environmental and mechanical wear and tear. As the fault continues, the cable insulation deteriorates, exacerbating the problem. Ground faults can occur in submarine cables when ships anchor and sever one of the lines. When it comes to overhead lines, illumination or construction work can cause a cut line to fall to the ground [40, 41]. The issue is permanent in all of these circumstances, and the line must be totally isolated before the cable can be replaced.

4.2.2 Pole-to-Pole Fault

Pole-to-pole faults are less common than line-to-ground faults. Due to the distance between the lines, it is extremely rare that an object will fall and cut both the positive and negative lines at the same time, resulting in a short circuit via the ground. A bipolar fault cannot be caused by lightning, especially in overhead lines. [40]. Undersea cables are almost impervious to such faults because they are frequently separated from one another and are well shielded by numerous layers of insulation and conduit, making the possibility of a simultaneous failure that would bring both conductors into contact less likely. Only in the event of a switching fault or failure at the converter station, which could result in a short circuit between the two poles, is a pole-to-pole fault more likely.

4.3 DC Fault Analysis

For both types of studied faults, a more detailed analysis is presented in this section. For a better understanding of the entire system reaction, the theoretically expected VSC system behavior is described. The DC fault analysis is shown in Chap. 5's simulation findings.

4.3.1 Pole-to-Pole Fault

When a pole-to-pole DC fault develops, the DC capacitors are rapidly discharged, causing the DC-link voltage to drop to zero and the DC current to swiftly grow to a high level. The DC capacitors' discharging current does not pass through the DSs or stack, hence there is no harm to the IGBTs or diodes. Because of the free-wheeling effects of the anti-parallel diodes, the AC-side currents flow directly into the DC fault site if the stacks do not supply reverse voltages against the AC-side currents, and the DC fault becomes an AC-side short circuit fault, as illustrated in Fig. 4.2. The growing AC-side short-circuit fault current runs through the stacks and DSs, potentially causing damage to the power electronic equipment [42].

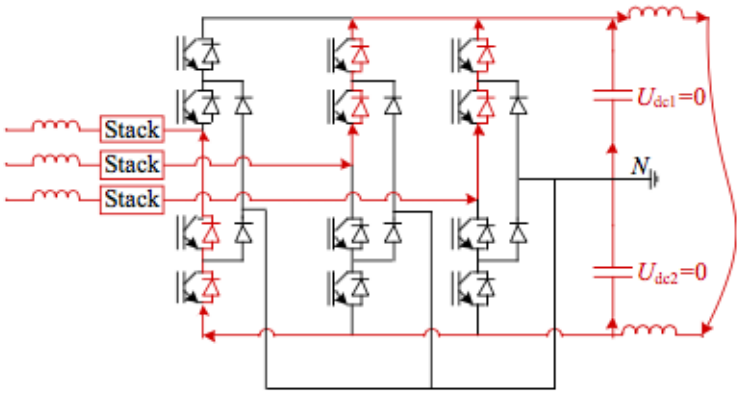

Figure 4.2: VSC with cable pole-to-ground fault state.

4.3.2 Pole-to-Ground Fault

The pole-to-ground fault has a similar mechanism to the pole-to-pole fault. As an example, the positive pole-to-ground fault is used. The upper DC capacitor is discharged once the DC fault occurs, and the positive-pole DC current rapidly grows to a high level, as shown in Fig. 4.3 [43].The upper DC capacitor's discharging current does not pass via the DSs or stacks, so the IGBTs and diodes are unaffected. The AC-side currents, on the other hand, flow through the stacks and DSs and into the DC fault location. The AC-side currents will rapidly increase if the stacks do not provide reverse voltages, potentially damaging the power electronic components.

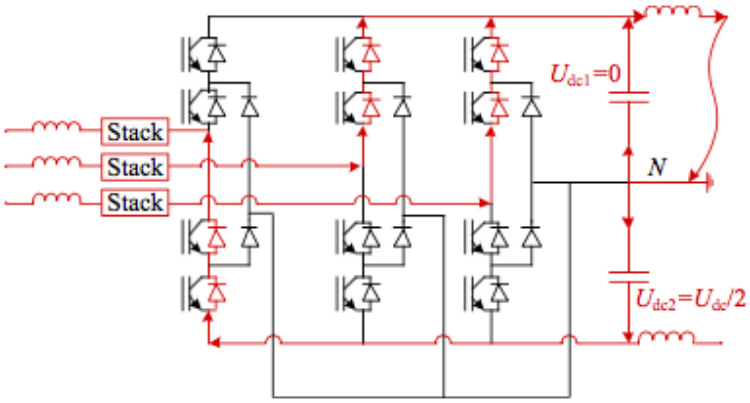

Figure 4.3: VSC with cable pole-to-pole fault state.

4.4 Conclusion

This chapter has highlighted the faults on the DC system. Pole-to-Pole and Pole-to-Ground faults were discussed. Pole-to-pole faults are considered as more severe due to the fact that they force the system to collapse, but they are less likely to occur. On the other hand pole- to-ground faults are less harmful but more likely to happen. Pole-to-pole faults are easier to detect but much more challenging to isolate successfully as they require very fast disconnection, while pole-to-ground faults (especially high resistive faults) pose less of a threat to the inverters (longer disconnection could be per- mitted), but harder to detect/discriminate.

Chapter 5

Simulation

5.1 Introduction

Figure 5.1 depicts the system under consideration in this thesis . The HVDC system is made up of two VSCs linked by a DC link. The converter VSC-1 is controlled by DC voltage control, whereas the converter VSC-2 is controlled by active power control. The transient behavior of control methods under normal and fault conditions for a VSC-based HVDC connected to a grid is investigated in this chapter. Vector current control is employed as the control method because it allows for independent regulation of active and reactive power.

5.2 Simulation and results discussion

To examine the performance of VSC-HVDC using vector current control system shown in Fig. 5.1 is implemented in SIMULINK using the parameters of Table 5.1. The obtained results are following:

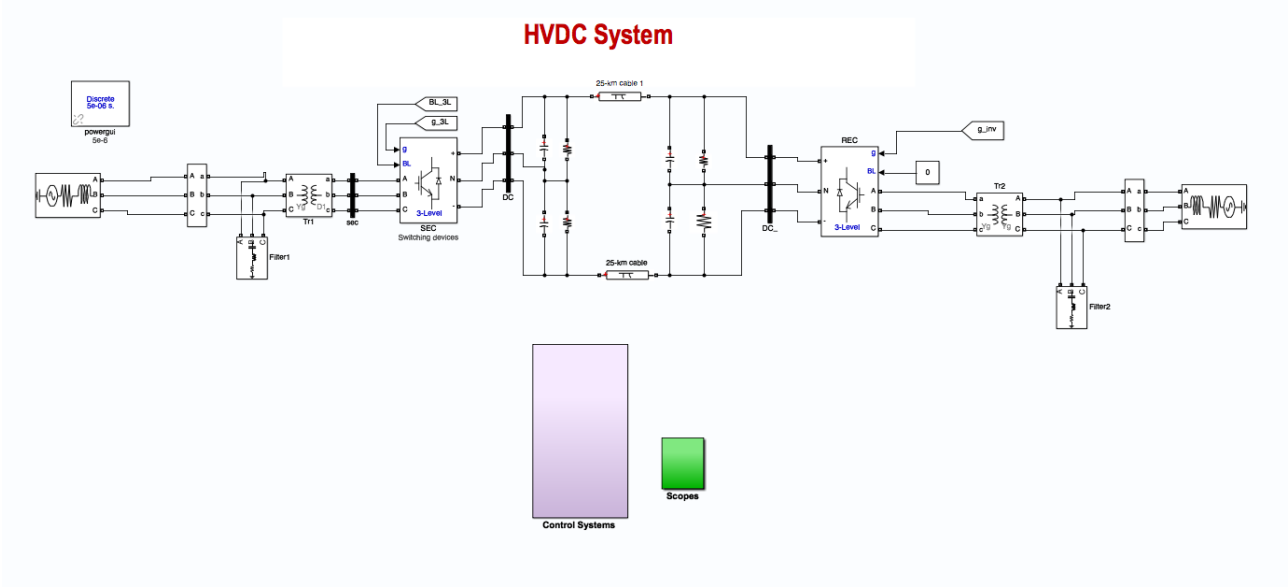

Figure 5.1: Test system under consideration, MATLAB/Simulink.

Parameters	Rating
Frequency (f)	50 Hz
DC voltage (U_{DC})	3000 V
AC voltage (V_n)	50 KVrms
Rated power (P)	3 MW
Switching frequency	50 MHz
Transmission length	25 Km

Table 5.1: Specifications of VSC used in the simulation

5.2.1 Part 1: Control Performance

DC voltage:

In Fig. 5.2 we can notice that our DC voltage wave-form follow the same path as the reference voltage. As shown in the Figure below, the DC voltage wave-form increases from 2800 v to 3000 v at t = 1s following its reference, so the DC voltage has a good tracking for its reference.

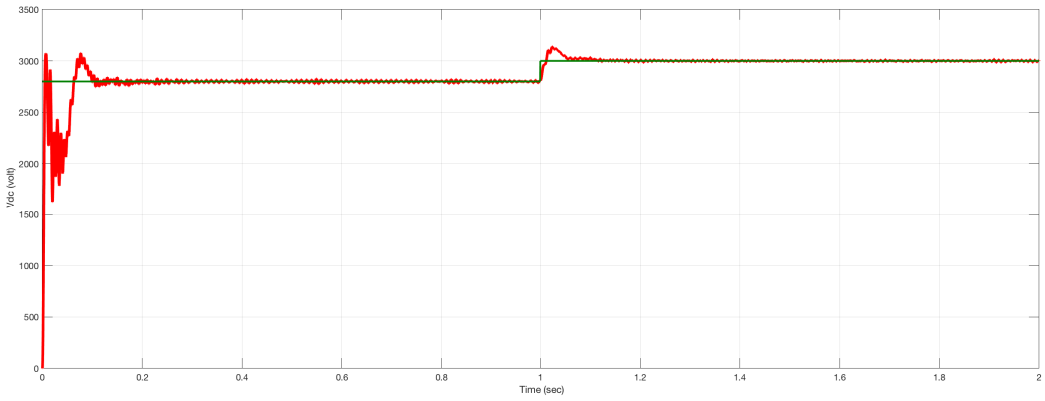

Figure 5.2: DC voltage and control responses.

Active and Reactive Power:

As it is presented in Fig. 5.3 and 5.4, the active and reactive power has follow the same path and has a good tracking capability for its current control signals id and iq respectively. At t = 1s, the active power increases following its reference control signal id increment which means that the system has a good response tracking capability. The Fig. 5.5 shows the active and reactive power of the converter's second side (VSC2) and as we can notice that at t = 1s the active power of this side decreases because there is an exchange of power to the rectifier side (VSC1).

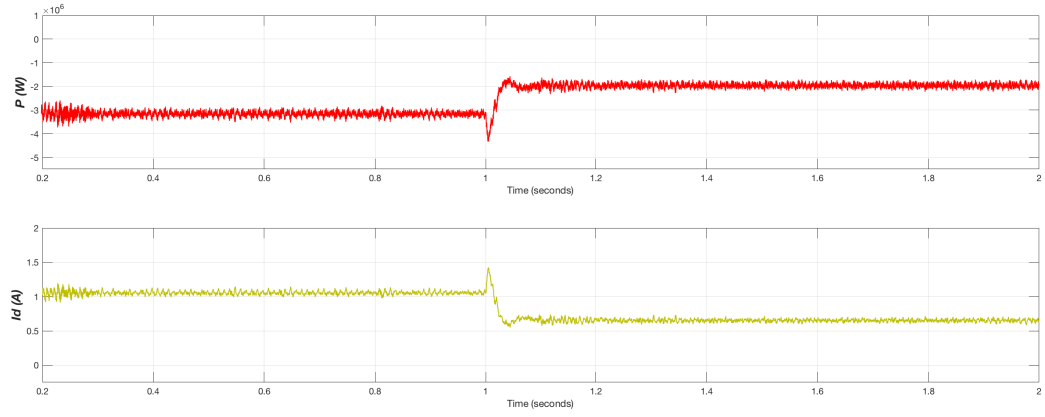

Figure 5.3: Active power control response with different changes.

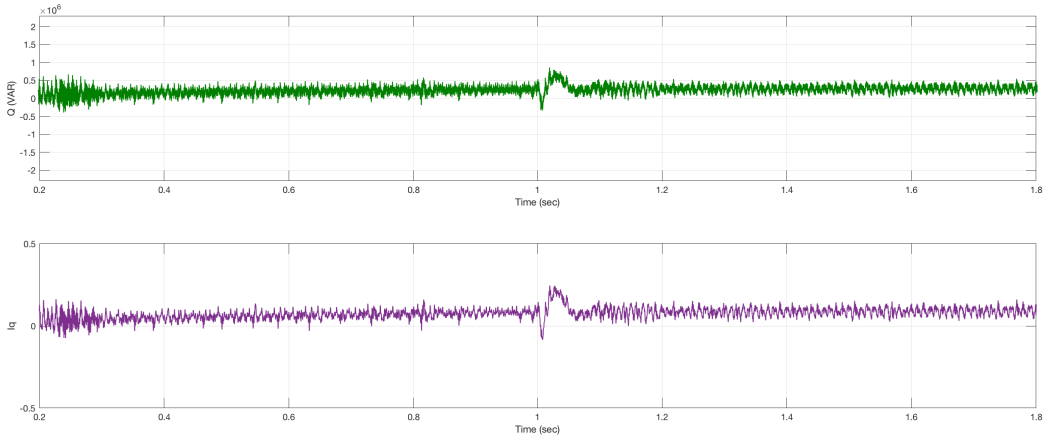

Figure 5.4: Reactive power control response with different changes.

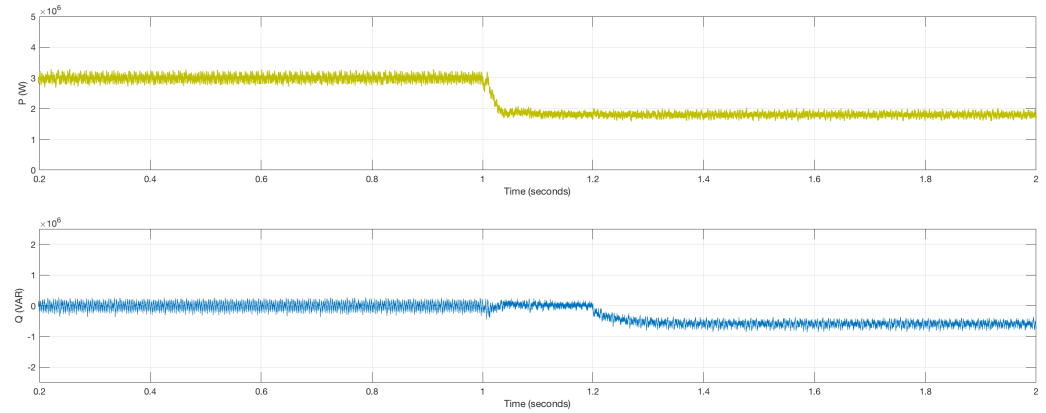

Figure 5.5: Active and Reactive Power of VSC2 side.

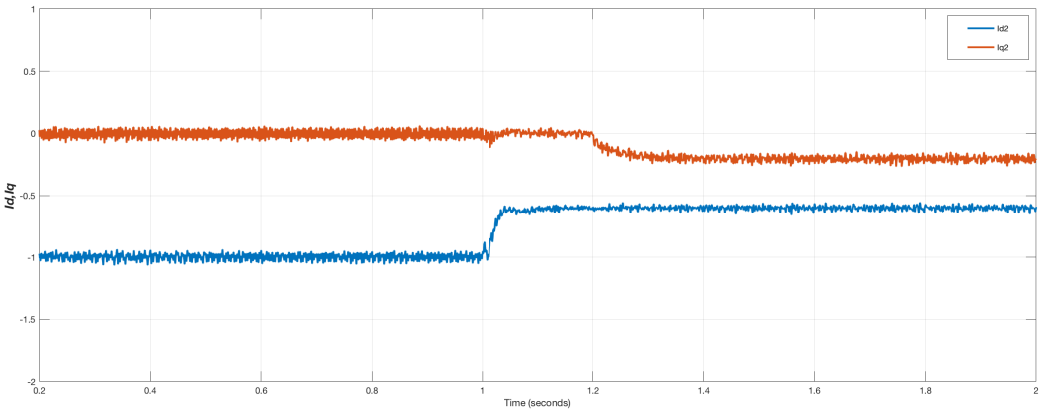

Figure 5.6: Current references of VSC2 side.

5.2.2 Part 2: Steady-State simulation

Results of voltage and current:

Both voltages and currents of VSC1 and VSC2 under steady-state operation are presented in Fig. 5.7 and 5.8, we can observe that the results at the inverter and rectifier side are almost the same. It can be seen from the figures mentioned above that the peak value of the current is around 40 A and the magnitude of the voltage is around 40 kVrms. Under no fault or disturbance conditions the phase angle between the grid phase voltage and current is the same but some distortion in the current wave-form. For the Fig. 5.8 shows the voltage at the inverter side.

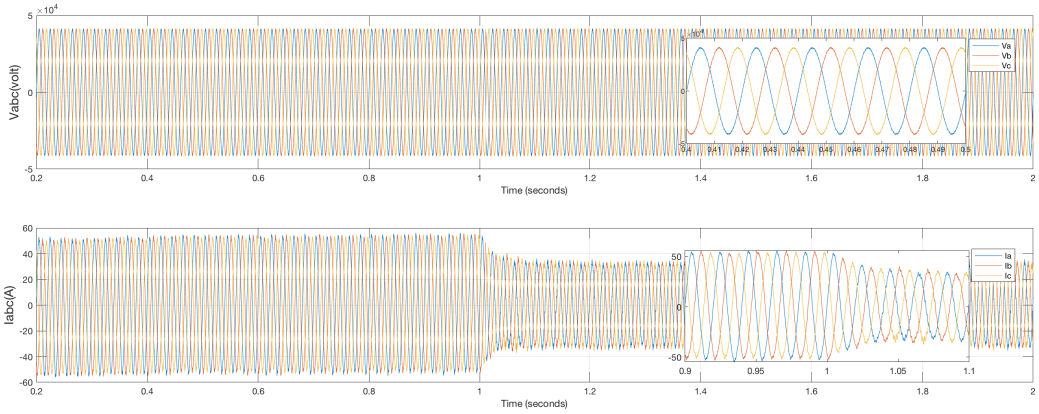

Figure 5.7: Voltage and current waveforms for VSC1.

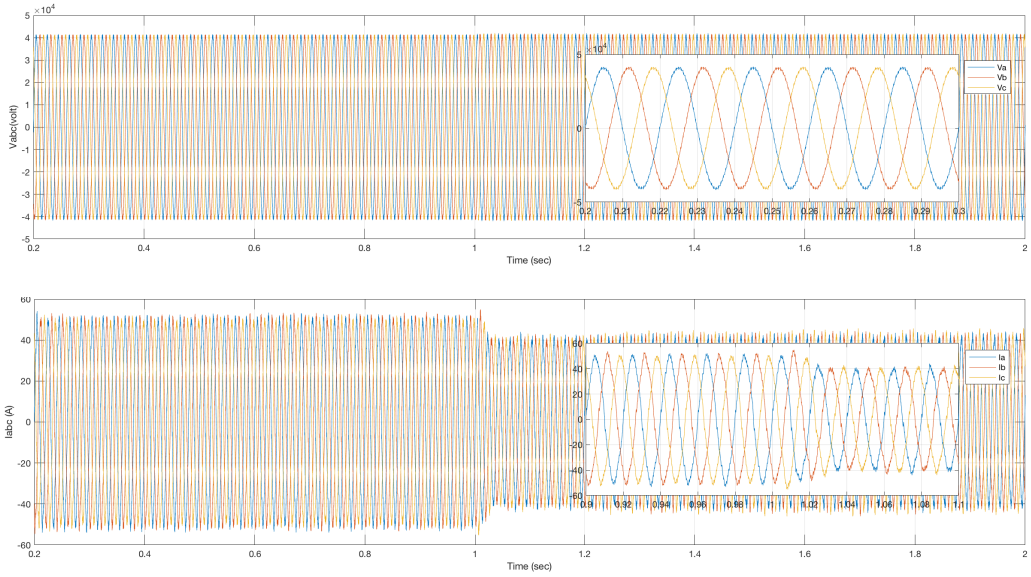

Figure 5.8: Voltage and current waveforms for VSC2.

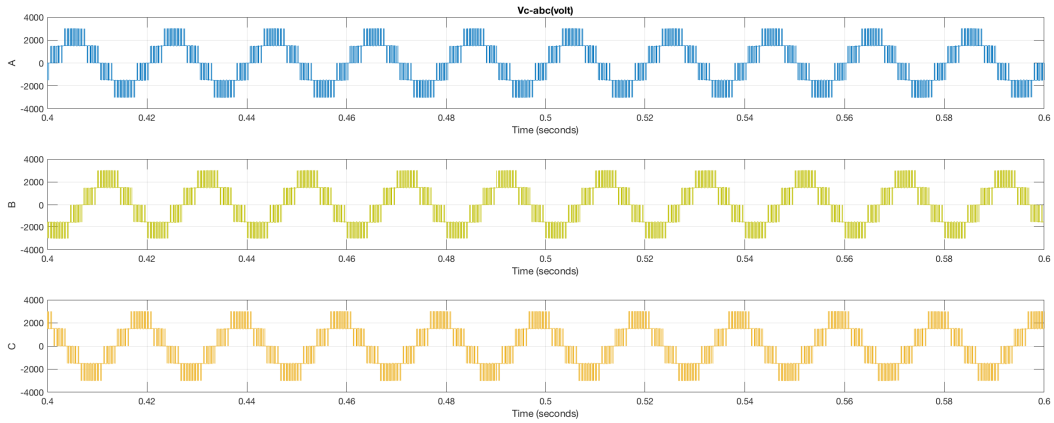

Figure 5.9: Voltage of the Inverter.

The Fig. 5.9 shows the voltage of the inverter.

5.2.3 Fast Fourier Transform (FFT) results:

The harmonic content of the planned VSC systems is evaluated using the current wave-form under steady-state operation. To estimate the harmonic magnitude of the line current, the Fast Fourier Transform (FFT) and the Total Harmonic Distortion (THD) blocks are used. The harmonic spectrum and the wave-form of the grid current of phase-a for the inverter is shown in Fig. 5.10, as we can observe, the THD is 2.6 % and this good result is due to the LC filter.

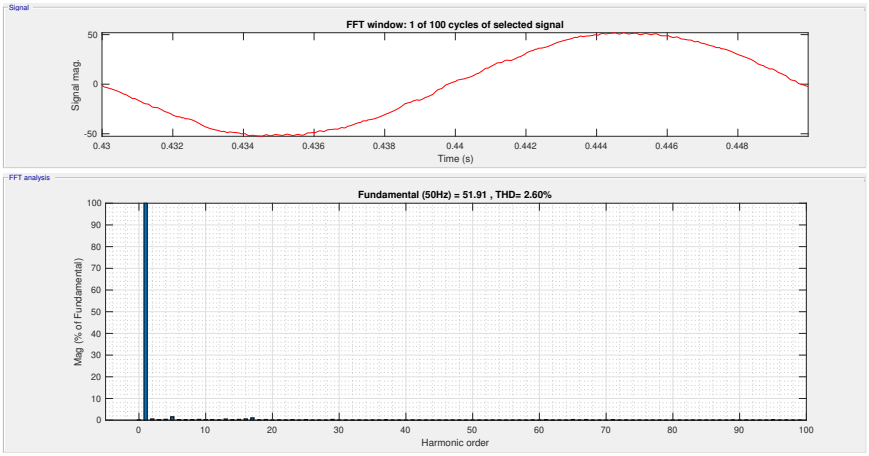

Figure 5.10: Harmonic spectrum of injected current at converter terminal , (a) individual harmonic distortion (%), (b) total harmonic distortion THD.

5.3 Part 3: Fault Results

5.3.1 Pole-to-Pole Fault

As shown in Fig. 5.11 and 5.12, at t = 1.5s a pole-to-pole fault has occurred, from the figures we can notice that the DC voltage instantaneously decreases from 3000 V to 0 V, and at the other hand at the same moment we have an instantaneous increment of the DC current to its maximum value 280 KA.

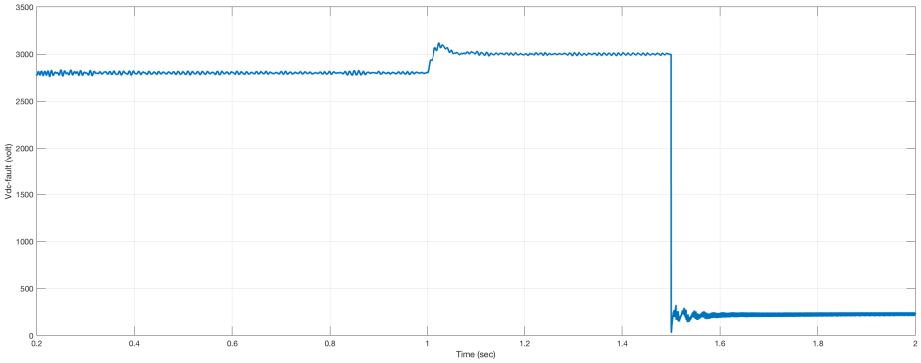

Figure 5.11: DC-link voltag.

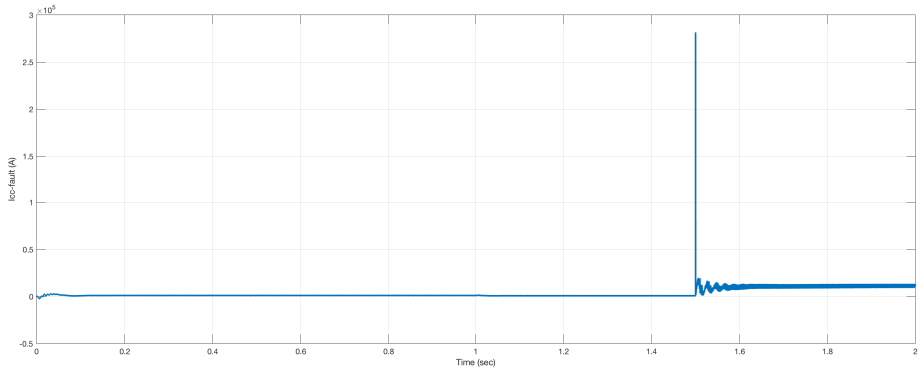

Figure 5.12: DC-link current.

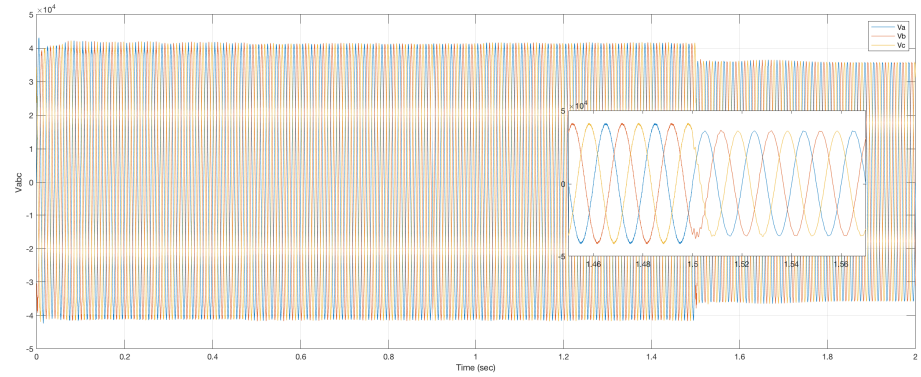

Figure 5.13: Grid-side voltage under fault.

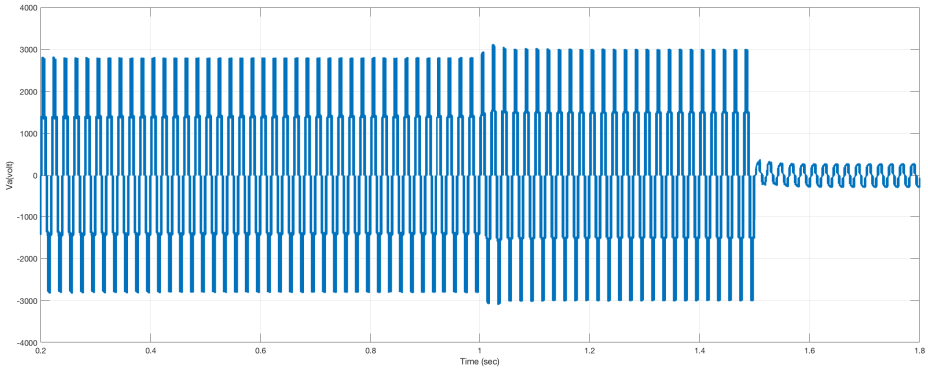

Figure 5.14: Inverter voltage under fault.

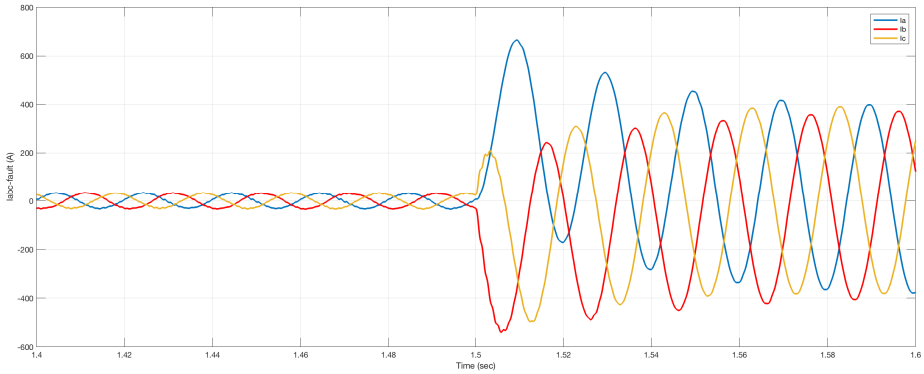

Figure 5.15: Grid-side currents.

Chapter 6

Conclusions and Future Work

6.1 Conclusions

The expanding relevance of VSC HVDC systems in the current grid, combined with its essential role in the vision of the future grid, calls for a substantial study effort to fully comprehend all elements linked to the operation of AC/DC grids. This work addresses this vital need by proposing a detailed study about the modelling and control of the VSC HVDC system. Power electronic switches governed by fast-acting control systems are at the heart of VSC HVDC systems.

VSC-HVDC systems offer various advantages compared to the LCC-HVDC system. One significant aspect is that the VSC-HVDC system can be connected to very weak ac systems where the LCC-HVDC system has issues. In this thesis, a detailed VSC HVDC model is derived starting from the basic mathematical Equations. A review of the different control strategies of VSC-based HVDC is carried out. The behaviour of the point-to-point VSC-based DC system under most critical DC pole-to-pole and pole-to-ground faults are studied. The following are the study's principal conclusions:

- Due to its fundamentally superior technical and grid-support capabilities compared to LCC-HVDC, VSC-HVDC transmission technology is beginning to dominate the market in projects rated at 2000MW or less, which is expected to continue for the foreseeable future.
- The HVDC transmission system controller is open or flexible that it is not merely dependent on a protection scheme like an HVAC system. The design of HVDC is improved with the applications of the VSC and the appropriate selection of control parameters.
- Control and system response performance are tested and validated under steady-state and fault conditions. Further, the design and control responses exhibit an excellent alignment.
- DC Pole-to-pole faults are seen as more severe since they push the system to collapse. That's the reason why we chose this type of fault for analysis.
- MATLAB/Simulink was used to simulate and test a complete VSC-HVDC transmission system in both normal and fault conditions.
- It is possible to control both active and reactive power without interfering with each other.

6.2 Suggestions for Future Work

The following points should be considered for future research in this area:
1.To support the findings presented in this thesis, experimental verification of the theoretical derivations and simulation results is required.
2.Control and implementation of MMC(Mulit-module converter) based HVDC system under fault condition.
3.The execution of the HVDC system using real-time simulation package.
4.Fault analysis and protection system design for HVDC grid.
5.Modelling, control system design and simulation of hybrid LCC-VSC HVDC system.

Appendix A

Transformations for three-phase systems

A.1 Introduction

In this appendix, the necessary transformations from three-phase quantities into vectors in stationary $\alpha\beta$ and rotating dq reference frames and vice versa will be described.

A.2 Transformation of three-phase quantities to vectors

A three phase system constituted by three quantities $v_a(t)$, $v_b(t)$, $v_c(t)$ can be transformed into a vector $\underline{v}^{(\alpha\beta)}(t)$ in a stationary complex reference frame, usually called $\alpha\beta$-frame, by applying the following transformation:

$$\underline{v}^{(\alpha\beta)}(t) = v^{\alpha}(t) + jv^{\beta}(t) = K_{tran}(v_a(t) + v_b(t)e^{j\frac{2}{3}\pi} + v_c(t)e^{j\frac{4}{3}\pi}) \tag{A.1}$$

The transformation constant K_{tran} can be choosen to be $\sqrt{2/3}$ or $2/3$ to ensure power invariant or amplitude invariant transformation respectively between the two systems. This thesis considers a power invariant transformation. Equation (A.1) can be expressed in matrix form as

$$\begin{bmatrix} v^{\alpha}(t) \\ v^{\beta}(t) \end{bmatrix} = \mathbf{T}_{32} \begin{bmatrix} v_a(t) \\ v_b(t) \\ v_c(t) \end{bmatrix} \tag{A.2}$$

where the matrix $\mathbf{T}_{32}$ is given by

$$\mathbf{T}_{32} = K_{tran} \begin{bmatrix} 1 & -\frac{1}{2} & -\frac{1}{2} \\ 0 & \frac{\sqrt{3}}{2} & -\frac{\sqrt{3}}{2} \end{bmatrix}$$

The inverse transformation, assuming no zero-sequence, i.e. $v_a(t) + v_b(t) + v_c(t) = 0$, is

given by the relation

$$\begin{bmatrix} v_a(t) \\ v_b(t) \\ v_c(t) \end{bmatrix} = \mathbf{T}_{23} \begin{bmatrix} v^{\alpha}(t) \\ v^{\beta}(t) \end{bmatrix} \tag{A.3}$$

where the matrix $\mathbf{T}_{23}$ is given by

$$\mathbf{T}_{23} = \frac{1}{K_{tran}} \begin{bmatrix} \frac{2}{3} & 0 \\ -\frac{1}{3} & \frac{1}{\sqrt{3}} \\ -\frac{1}{3} & -\frac{1}{\sqrt{3}} \end{bmatrix}$$

A.2.1 Transformation between fixed and rotating coordinate systems

For the vector $\underline{v}^{(\alpha\beta)}(t)$ rotating in the $\alpha\beta$ with the angular frequency $w(t)$ in the positive (counter-clockwise direction), a dq-frame that rotates in the same direction with the same angular frequency $w(t)$ can be defined. The vector $\underline{v}^{(\alpha\beta)}(t)$ will appear as fixed vectors in this rotating reference frame. A projection of the vector $\underline{v}^{(\alpha\beta)}(t)$ on the d-axis and q-axis of the dq-frame gives the components of the vector on the dq-frame as illustrated in Fig. A.1.

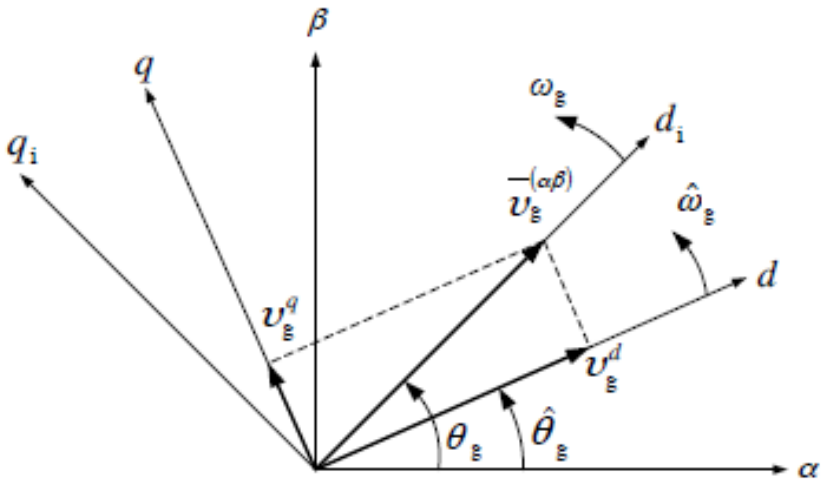

Figure A.1: Relation between $\alpha\beta$-frame and dq-frame..

The transformation can be written in vector form as follows

$$\underline{v}^{(dq)}(t) = v^d(t) + jv^q(t) = \underline{v}^{(\alpha\beta)}(t)e^{-j\theta(t)} \tag{A.4}$$

with the angle $\theta(t)$ in Fig. A.1 given by

$$\theta(t) = \theta_0 + \int_0^t w(\tau)d\tau$$

The inverse transformation, from the rotating d-frame to the fixed $\alpha\beta$-frame, is provided as

$$\underline{v}^{(\alpha\beta)}(t) = \underline{v}^{(dq)}(t)e^{j\theta(t)} \tag{A.5}$$

In matrix form, the transformation between the fixed $\alpha\beta$-frame and the rotating dq-frame can be written as

$$\begin{bmatrix} v^d(t) \\ v^q(t) \end{bmatrix} = \mathbf{R}(-\theta(t)) \begin{bmatrix} v^\alpha(t) \\ v^\beta(t) \end{bmatrix} \tag{A.6}$$

$$\begin{bmatrix} v^\alpha(t) \\ v^\beta(t) \end{bmatrix} = \mathbf{R}(\theta(t)) \begin{bmatrix} v^d(t) \\ v^q(t) \end{bmatrix} \tag{A.7}$$

where the projection matrix is

$$\mathbf{R}(\theta(t)) = \begin{bmatrix} \cos(\theta(t)) & -\sin(\theta(t)) \\ \sin(\theta(t)) & \cos(\theta(t)) \end{bmatrix} \tag{A.8}$$

References

[1] Jon Moore and Seb Henbest. New energy outlook 2020, executive summary. *BloombergNEF (New Energy Finance). Available online: https://assets. bbhub. io/professional/sites/24/928908_NEO2020-Executive-Summary. pdf (accessed on 9 November 2020).*

[2] Abdulrahman Alassi, Santiago Bañales, Omar Ellabban, Grain Adam, and Callum MacIver. Hvdc transmission: technology review, market trends and future outlook. *Renewable and Sustainable Energy Reviews*, 112:530–554, 2019.

[3] E Abiri, A Rahmati, and A Abrishamifar. A sensorless and simple controller for vsc based hvdc systems. *Journal of Zhejiang University-Science A*, 10(12):1824–1834, 2009.

[4] H Wayne Beaty and Donald G Fink. *Standard handbook for electrical engineers*. McGraw-Hill Education, 2013.

[5] Hendrik Rissik. *Mercury-arc Current Convertors: An Introduction to the Theory and Practice of Vapour-arc Discharge Devices and to the Study of Rectification Phenomena*. Sir I. Pitman & sons, Limited, 1941.

[6] A Kalair, N Abas, and N Khan. Comparative study of hvac and hvdc transmission systems. *Renewable and Sustainable Energy Reviews*, 59:1653–1675, 2016.

[7] Stijn Cole and Ronnie Belmans. Transmission of bulk power. *IEEE Industrial Electronics Magazine*, 3(3):19–24, 2009.

[8] COLE Stijn. *Steady-state and dynamic modelling of VSC HVDC systems for power system Simulation*. PhD thesis, Ph. D. dissertation, PhD dissertation, Katholieke University Leuven, Belgium, 2010.

[9] Martial Giraneza. *High voltage direct current (HVDC) in applications for distributed independent power providers (IPP)*. PhD thesis, Cape Peninsula University of Technology, 2013.

[10] Mircea Ardelean and Philip Minnebo. Hvdc submarine power cables in the world. *Joint Research Center*, 2015.

[11] Hasan Alsiraji. Cooperative power sharing control in multi-terminal vsc-hvdc. Master's thesis, University of Waterloo, 2014.

[12] Erika Pierri, Ole Binder, Nasser GA Hemdan, and Michael Kurrat. Challenges and opportunities for a european hvdc grid. *Renewable and Sustainable Energy Reviews*, 70:427–456, 2017.

[13] Gesong Chen, Xiaoxin Zhou, and Rui Chen. *Variable Frequency Transformers for Large Scale Power Systems Interconnection: Theory and Applications*. John Wiley & Sons, 2018.

[14] B Ronner, P Maibach, and T Thurnherr. Operational experiences of statcoms for wind parks. *IET Renewable Power Generation*, 3(3):349–357, 2009.

[15] MP Bahrman. Hvdc transmission overview. In *2008 IEEE/PES Transmission and Distribution Conference and Exposition*, pages 1–7. IEEE, 2008.

[16] http://www.nsenergybusiness.com/.

[17] Amirnaser Yazdani and Reza Iravani. *Voltage-sourced converters in power systems: modeling, control, and applications*. John Wiley & Sons, 2010.

[18] Nikolas Flourentzou, Vassilios G Agelidis, and Georgios D Demetriades. Vsc-based hvdc power transmission systems: An overview. *IEEE Transactions on power electronics*, 24(3):592–602, 2009.

[19] Nagwa F Ibrahim and Sobhy S Dessouky. *Design and Implementation of Voltage Source Converters in HVDC Systems*. Springer, 2021.

[20] B Chuco and EH Watanabe. A comparative study of dynamic performance of hvdc system based on conventional vsc and mmc-vsc. In *2010 IREP Symposium Bulk Power System Dynamics and Control-VIII (IREP)*, pages 1–6. IEEE, 2010.

[21] MA Djehaf, SA Zidi, YI Djilani Kobibi, and S Hadjeri. Modeling of a multi-level converter based vsc hvdc supplying a dead load. In *2015 International Conference on Electrical and Information Technologies (ICEIT)*, pages 218–223. IEEE, 2015.

[22] AG Siemens. Robicon perfect harmony, 2016.

[23] Mohamed H Okba, Mohamed H Saied, MZ Mostafa, and TM Abdel-Moneim. High voltage direct current transmission-a review, part i. In *2012 IEEE Energytech*, pages 1–7. IEEE, 2012.

[24] Michael Bahrman and Per-Erik Bjorklund. The new black start: system restoration with help from voltage-sourced converters. *IEEE Power and Energy Magazine*, 12(1):44–53, 2013.

[25] G Shilpa and Premila Manohar. Hybrid hvdc system for multi-infeed applications. In *2013 International Conference on Emerging Trends in Communication, Control, Signal Processing and Computing Applications (C2SPCA)*, pages 1–5. IEEE, 2013.

[26] Georgios Stamatiou. *Analysis of VSC-based HVDC systems*. Chalmers Tekniska Hogskola (Sweden), 2016.

[27] Cuiqing Du. *The control of VSC-HVDC and its use for large industrial power systems*. Chalmers Tekniska Hogskola (Sweden), 2003.

[28] Grain P Adam, Khaled H Ahmed, Stephen J Finney, and Barry W Williams. Modular multilevel converter for medium-voltage applications. In *2011 IEEE International Electric Machines & Drives Conference (IEMDC)*, pages 1013–1018. IEEE, 2011.

[29] Lie Xu and Liangzhong Yao. Dc voltage control and power dispatch of a multi-terminal hvdc system for integrating large offshore wind farms. *IET renewable power generation*, 5(3):223–233, 2011.

[30] Temesgen Mulugeta Haileselassie. Control, dynamics and operation of multi-terminal vsc-hvdc transmission systems. 2012.

[31] Dragan Jovcic. *High voltage direct current transmission: converters, systems and DC grids*. John Wiley & Sons, 2019.

[32] Shuxin Luo, Xinzhou Dong, Shenxing Shi, and Bin Wang. A directional protection scheme for hvdc transmission lines based on reactive energy. *IEEE transactions on Power Delivery*, 31(2):559–567, 2015.

[33] Javier Renedo Anglada, Aurelio García Cerrada, and Luis Rouco Rodríguez. Reactive-power coordination in vsc-hvdc multi-terminal systems for transient stability improvement. 2017.

[34] Yong Li, Longfu Luo, Christian Rehtanz, Sven Rüberg, and Fusheng Liu. Realization of reactive power compensation near the lcc-hvdc converter bridges by means of an inductive filtering method. *IEEE transactions on power electronics*, 27(9):3908–3923, 2012.

[35] MA Hannan, I Hussin, Pin Jern Ker, Md Murshadul Hoque, MS Hossain Lipu, Aini Hussain, MS Abd Rahman, CWM Faizal, and Frede Blaabjerg. Advanced control strategies of vsc based hvdc transmission system: Issues and potential recommendations. *IEEE Access*, 6:78352–78369, 2018.

[36] Lennart Harnefors, Massimo Bongiorno, and Stefan Lundberg. Input-admittance calculation and shaping for controlled voltage-source converters. *IEEE transactions on industrial electronics*, 54(6):3323–3334, 2007.

[37] Lennart Harnefors and H-P Nee. Model-based current control of ac machines using the internal model control method. *IEEE Transactions on Industry Applications*, 34(1):133–141, 1998.

[38] Mebtu Beza. *Control of energy storage equipped shunt-connected converter for electric power system stability enhancement*. Chalmers Tekniska Hogskola (Sweden), 2012.

[39] Lennart Angquist and Massimo Bongiorno. Auto-normalizing phase-locked loop for grid-connected converters. In *2009 IEEE Energy Conversion Congress and Exposition*, pages 2957–2964. IEEE, 2009.

[40] Ke Ma, Wenjie Chen, Marco Liserre, and Frede Blaabjerg. Power controllability of a three-phase converter with an unbalanced ac source. *IEEE Transactions on Power Electronics*, 30(3):1591–1604, 2014.

[41] Tao Jing and Alexander S Maklakov. A review of voltage source converters for energy applications. In *2018 International Ural Conference on Green Energy (UralCon)*, pages 275–281. IEEE, 2018.

[42] Matthias K Bucher and Christian M Franck. Analytic approximation of fault current contribution from ac networks to mtdc networks during pole-to-ground faults. *IEEE Transactions on Power Delivery*, 31(1):20–27, 2015.

[43] Jin Yang, John E Fletcher, and John O'Reilly. Short-circuit and ground fault analyses and location in vsc-based dc network cables. *IEEE transactions on Industrial Electronics*, 59(10):3827–3837, 2011.

[44] Sul Ademi, Dimitrios Tzelepis, Adam Dysko, Sankara Subramanian, and Hengxu Ha. Fault current characterisation in vsc-based hvdc systems. 2016.